Journal of
Mechanics of
Materials and Structures

ASYMPTOTIC STRESS FIELD IN THE VICINITY OF A MIXED-MODE CRACK UNDER PLANE STRESS CONDITIONS FOR A POWER-LAW HARDENING MATERIAL

Larisa V. Stepanova and Ekaterina M. Yakovleva

Volume 10, No. 3 May 2015

msp

JOURNAL OF MECHANICS OF MATERIALS AND STRUCTURES
Vol. 10, No. 3, 2015
dx.doi.org/10.2140/jomms.2015.10.367

msp

ASYMPTOTIC STRESS FIELD IN THE VICINITY OF A MIXED-MODE CRACK UNDER PLANE STRESS CONDITIONS FOR A POWER-LAW HARDENING MATERIAL

LARISA V. STEPANOVA AND EKATERINA M. YAKOVLEVA

The stress-strain state analysis near the crack tip in a power-law material under mixed-mode loading conditions is investigated. By the use of the eigenfunction expansion method the stress-strain state near the mixed-mode crack tip under plane stress conditions is found. The type of the mixed-mode loading is specified by the mixity parameter, which varies from 0 to 1. The value of the mixity parameter corresponding to a mode II crack loading is equal to 0, whereas the value corresponding to a mode I crack loading is equal to 1. It is shown that the eigenfunction expansion method results in a nonlinear eigenvalue problem. The numerical solutions of the nonlinear eigenvalue problems for all values of the mixity parameter and for all practically important values of the strain hardening (or creep) exponent are obtained. It is found that mixed-mode loading of the cracked plate gives rise to a change in the stress singularity in the vicinity of the crack tip. Mixed-mode loading of the cracked plate results in new asymptotics of the stress field, which is different from the classical Hutchinson–Rice–Rosengren (HRR) stress field. The approximate solution of the nonlinear eigenvalue problem is obtained by a perturbation theory technique (artificial small parameter method). In the framework of the perturbation theory approach, a small parameter representing the difference between the eigenvalue of the nonlinear problem and the undisturbed linear problem is introduced. The asymptotic analysis carried out shows clearly that the stress singularity in the vicinity of the crack tip changes under mixed-mode loading in the case of plane stress conditions. The angular distributions of the stress and strain components (eigenfunctions) in the full range of values of the mixity parameter are given.

1. Introduction. Mixed-mode loading of cracked structures and near crack-tip fields under mixed-mode loading.

Knowledge of stress, strain and displacement fields in the vicinity of the crack tip under mixed-mode loading conditions is important for the justification of fracture mechanics criteria and has attracted considerable attention [Berto and Lazzarin 2014; Bui 2011; Kuna 2013; Pestrikov and Morozov 2012; Vildeman et al. 2012; Wei 2010]. So far, mainly crack problems for pure opening mode I at symmetrical loading have been thoroughly treated [Bui 2006; Wei 2010; Pestrikov and Morozov 2012]. The corresponding fracture criteria have been obtained on the assumption that the crack continues to extend along its original line (two-dimensional case) or plane (three-dimensional case) in a straightforward manner on the ligament. If mode I loading is superimposed with mode II and/or III loading, the symmetry is violated and the situation is called mixed-mode loading. Stress fields around a mixed-mode crack tip in

The authors would like to acknowledge the financial support of the Russian foundation of basic research, project 13-01-97009-a.
Keywords: stress-strain state near the crack tip, mixed-mode loading, mixity parameter, nonlinear eigenvalue problem, perturbation technique.

different materials have been investigated by many researchers [Dong and Pan 1990; Smith et al. 2001; Shlyannikov 2003; Pan and Lin 2006; Shlyannikov and Kislova 2009; Rahman and Hancock 2006; Berto and Lazzarin 2013; Berto and Lazzarin 2014; Leblond and Frelat 2014; Akbardoost and Ayatollahi 2014]. The study of mixed-mode loads is of particular importance: mixed-mode loading of cracked specimens is of profound importance from theoretical [Bui 2011; Pestrikov and Morozov 2012; Wei 2010], computational [Kuna 2013] and experimental [Decreuse et al. 2012; Ondraček and Materna 2014; Vildeman et al. 2012; Wei et al. 2011] points of view. Currently, mixed-mode crack problems in materials with nonlinear constitutive relations (power law constitutive equations of deformation plasticity theory, steady state creep Norton's law) have aroused considerable interest in many areas of fracture mechanics [Berto and Lazzarin 2013; Botvina et al. 2013; Hello et al. 2012; Richard et al. 2014; Shlyannikov and Kislova 2009; Shlyannikov 2012; 2013; Shlyannikov and Zakharov 2014; Shlyannikov et al. 2014]. Obviously, the principle of superposition of the solutions for mode I and mode II loadings cannot be applied for nonlinear materials. For the case of nonlinear material behavior it is necessary to propose new methods and approaches for the analysis of the near crack tip stress-strain state under mixed-mode loads. In the present paper, the approximate analysis and numerical analysis of the stress and strain fields ahead of the crack tip under mixed-mode loading in the case of plane stress conditions are developed. It should be noted that the angular distributions and the stress singularity in the neighborhood of the crack tip under mixed-mode loading in the case of plane strain conditions are carefully studied [Loghin and Joseph 2001; 2003; Richard et al. 2014; Shlyannikov and Kislova 2009; Shlyannikov 2012].

Loghin and Joseph [2001] were the first to propose a displacement-based finite element formulation to determine the leading two terms in the expansions of stresses and strains around singular points in power law hardening materials. The authors used the approach to study the effects of mixed-mode loading on the structure. The asymptotic solution for mixed-mode loading of the cracked structure in plane strain conditions was obtained, but the asymptotic form of the mode I dominant plane stress could not be determined.

Shlyannikov and Kislova [2009] proposed a method for calculating the elastic-plastic stress intensity factors for the full range of mixed-mode loading from tensile to shear cracks. The state of an arbitrary oriented slit-like straight crack in the form of a mathematical notch under biaxial loading was considered. The solution is based on a combination of both the compatibility strain equation and the Airy stress potential with its derivatives. The elastic-plastic material behavior is represented by the Ramberg–Osgood model. On the basis of the results obtained, the influence of both mode-mixity and material plastic properties on the elastic-plastic stress intensity factors is analyzed. In [Richard et al. 2014], an overview of theories, experiments and simulations of cracks and crack growth under mixed-mode loading is given. First some concepts and basic theories are described for two-dimensional and three-dimensional crack mixed-mode loading situations. Furthermore, several mixed-mode fracture specimens and loading devices are presented. The theoretical and experimental results are compared with respect to practical use of the described concepts and theories. Finally, the paper [Richard et al. 2014] presents crack growth simulations. Shlyannikov [2012] derived equations for ultimate failure strain under complex static and low-cyclic loading and gave experimental verification for different types of biaxial loads. Experimental and calculation data obtained on the basis of a generalized equivalence condition to solve problems of crack mechanics for complex stress states are presented [loc. cit.]. Models and methods for determining the crack direction, path, velocity and time of crack growth under biaxial loading are

considered. Botvina et al. [2013] presented the results of studying the development of plastic flow zones and damage of steel 20 in conditions of shear, separation, mixed-mode loading and eccentric cyclic loading. The influence of the shear component on the evolution of plastic strain zones, mechanical and acoustic properties (parameters of acoustic emission, the velocity and attenuation of ultrasonic waves) is elucidated. It is shown that an increase in the shear component of the load changes the shape of the zone of plastic deformation, initiates formation of additional microcracks, increases the total fracture energy, reduces the slope indices of cumulative distributions of the amplitude of acoustic signals and microcracks, and also induces an increase in the ultrasonic attenuation coefficient and heat capacity of the samples. Analysis of changes in the studied parameters of damage and fracture mechanics provided identification of the main stages of damage accumulation under tensile load. The main aim of the study [Berto and Lazzarin 2013] is to present a set of equations for accurately describing the crack tip stress components, particularly for those cases where the modes I and II stress intensity factors, used in combination with the T-stress component, are unable to capture with satisfying precision the complete stress field ahead the crack tip. The case of a plate with a central crack under mixed-mode (I+II) loading is discussed to show the different contributions of the higher-order terms in the overall stress field. In [Berto and Lazzarin 2014], an extensive review of local approaches applicable near stress raisers, both sharp and blunt, for mode I, mode II and mode III loading conditions in brittle and quasibrittle failure assessment is presented. The authors develop a new approach based on the volume strain energy density and show many applications for assessment of the brittle fracture of a large number of materials and specimens under mixed-mode loading conditions. In [Hello et al. 2012] there are closed-form expressions for the whole sequences of coefficients related to the problem of a finite crack in an infinite plane medium with mode I and mode II remote load.

Fatigue crack paths for inclined cracks are studied in [Shlyannikov 2013] through experiments and computations under different mixed-mode loading conditions where the elaborated theoretical model is applied for modeling crack growth trajectories in common experimental fracture mechanics specimen geometries. For the particular specimen geometries considered, the T-stress distributions are calculated along the curved crack path. It is shown that there is a greater variation of T-stress along the crack trajectories under mixed-mode fracture for specimens with different geometries. The experimental results for mixed-mode fracture trajectories during crack growth are compared with theoretical predictions. Discrepancies in fatigue crack path have been observed in various specimen configurations. The results presented in this study for fracture specimens seem to indicate the relevance of the crack tip constraint parameter, the T-stress, to fatigue crack path behavior that traditional linear fracture mechanics fails to explain. In [Shlyannikov and Zakharov 2014], fatigue crack growth rate is analyzed through experimental study and numerical computations under different biaxial and mixed-mode loading conditions. Cruciform specimens under biaxial loading and compact tension-shear specimens are considered. The different degrees of mode mixity, from pure mode I to pure mode II, are given by combinations of the far-field stress level, load biaxiality and inclined crack angle. For the particular specimen geometries considered, the T-stress and the numerical constant of the plastic stress field distributions are obtained as a function of the dimensionless crack length, load biaxiality and mode mixity. The method is also suggested for calculating the plastic stress intensity factor for any mixed-mode I/II loading based on the T-stress and power law solutions. It is either demonstrated that the plastic stress intensity factor accounting for the in-plane and out-of-plane constraint effect can be used to characterize the multiaxial crack growth

rate for a variety of specimen geometries. Cruciform specimens of two configurations with an inclined crack subject to a system of biaxial loads are proposed [Shlyannikov et al. 2014] to study cracks under mixed-mode loading conditions. A method for infiltrating the mixed-mode displacement of cracks in the deformed state is suggested. For the particular specimen geometries considered, the T-stress and the geometry-dependent correction factors, as well as the numerical constant of the plastic stress distributions, are obtained as a function of the dimensionless crack length, load biaxiality and mode mixity.

Asymptotic representations of the stress, strain rate and continuity fields in the vicinity of the mixed-mode crack under plane strain conditions are obtained in [Stepanova and Adylina 2014]. On the basis of the similarity form of the solution and the hypothesis of the completely damaged zone in the crack tip region, the stress and continuity fields under a complete range of mixed-mode I/II states of loading (from pure tension to pure shear) are given. Higher-order term asymptotic expansions of the stress components and the continuity parameter are derived. A new numerical method to tackle nonlinear eigenvalue problems allowing one to find the whole spectrum of eigenvalues is proposed. However, several difficulties emerge in analyzing the nonlinear eigenvalue problem arising from the mixed-mode crack problem under plane stress conditions. The aim of the present study is to give an accurate solution of the nonlinear eigenvalue problem following from the stress-strain state analysis in the vicinity of the mixed-mode crack under plane stress conditions. It should be noted that plane stress state problems for notched bodies and cracked specimens are still not clearly understood. The angular distributions of the stress components in the vicinity of the mixed-mode crack tip under plane stress conditions have not been discussed in detail, but clearly this must be done to have an accurate description of the stress and strain fields in the vicinity of the crack tip. Recently there have been proposed solutions for the plane stress problems [Lomakin and Melnikov 2009; 2011; Vildeman et al. 2014]. The objective of this paper is to study the stress singularities in the vicinity of the mixed-mode crack tip under plane stress conditions. The governing equations for the power law constitutive relations are transformed to nonlinear eigenvalue problems of ordinary differential equations (ODEs) based on the assumption that the stress fields are asymptotic near the mixed-mode crack tip. The asymptotic and numerical methods are further developed in the present work to analyze eigenvalue problems of ODEs.

2. Governing equations and asymptotic analysis. Mixity parameter.

Consider a stationary crack in a power-law material under plane stress conditions. Applied loading is accounted as mixed-mode I/II loading. Polar coordinates are introduced and centered at the crack tip. With reference to the polar coordinates, the equilibrium equations can be written as

$$r\sigma_{rr,r} + \sigma_{r\theta,\theta} + \sigma_{rr} - \sigma_{\theta\theta} = 0, \quad r\sigma_{r\theta,r} + \sigma_{\theta\theta,\theta} + 2\sigma_{r\theta} = 0. \tag{2-1}$$

The compatibility condition has the form

$$2(r\varepsilon_{r\theta,\theta})_{,r} = \varepsilon_{rr,\theta\theta} - r\varepsilon_{rr,r} + r(r\varepsilon_{\theta\theta})_{,rr}. \tag{2-2}$$

For a material subjected to a power-law hardening, the constitutive equations for plane stress conditions can be written as

$$\varepsilon_{rr} = \tfrac{1}{2}B\sigma_e^{n-1}(2\sigma_{rr} - \sigma_{\theta\theta}), \quad \varepsilon_{\theta\theta} = \tfrac{1}{2}B\sigma_e^{n-1}(2\sigma_{\theta\theta} - \sigma_{rr}), \quad \varepsilon_{r\theta} = \tfrac{3}{2}B\sigma_e^{n-1}\sigma_{r\theta}, \tag{2-3}$$

where $\sigma_e = \sqrt{\sigma_{rr}^2 + \sigma_{\theta\theta}^2 - \sigma_{rr}\sigma_{\theta\theta} + 3\sigma_{r\theta}^2}$ is the von Mises equivalent stress, and B, n are the material constants.

It should be noted that in the case considered the analogy between nonlinear elastic behavior and creep holds. That implies that all relations and solutions obtained for a nonlinear elastic (plastic) material with the constitutive equations (2-3) can be transferred to creep processes with the constitutive relations of Norton's creep law simply by replacing the strains by strain rates. The solution of equations (2-1)–(2-3) should satisfy the traditional traction-free boundary conditions on the crack surfaces $\sigma_{r\theta}(r, \theta = \pm\pi) = 0$, $\sigma_{\theta\theta}(r, \theta = \pm\pi) = 0$. The mixed-mode loading can be characterized in terms of the mixity parameter M^p, which is defined as [Shih 1973; 1974]

$$M^p = (2/\pi)\arctan\left|\lim_{r\to 0}\frac{\sigma_{\theta\theta}(r, \theta = 0)}{\sigma_{r\theta}(r, \theta = 0)}\right|. \tag{2-4}$$

The mixity parameter M^p equals 0 for pure mode II, 1 for pure mode I, and $0 < M^p < 1$ for different mixities of modes I and II. Thus, for combined-mode fracture, the mixity parameter M^p completely specifies the near-crack-tip fields for a given value of the hardening exponent n. By postulating the Airy stress function $\chi(r, \theta)$ expressed in the polar coordinate system, the stress components in the plane strain and the plane stress states are expressed as

$$\sigma_{\theta\theta} = \chi_{,rr}, \quad \sigma_{rr} = \chi_{,r}/r - \chi_{,\theta\theta}/r^2, \quad \sigma_{r\theta} = -(\chi_{,\theta})_{,r}.$$

As for the asymptotic stress field at the crack tip $r \to 0$, one can postulate the Airy stress function

$$\chi(r, \theta) = Kr^{\lambda+1} f(\theta), \tag{2-5}$$

where K is an indeterminate coefficient, λ is an indeterminate exponent and $f(\theta)$ is an indeterminate function of the polar angle. In view of the asymptotic presentation (2-5), the asymptotic stress field at the crack tip is found to be $\sigma_{ij}(r, \theta) = Kr^{\lambda-1}\tilde{\sigma}_{ij}(\theta)$, or

$$\begin{aligned}
\sigma_{rr}(r, \theta) &= Kr^{\lambda-1}[(\lambda+1)f(\theta) + f''(\theta)],\\
\sigma_{\theta\theta}(r, \theta) &= Kr^{\lambda-1}(\lambda+1)\lambda f(\theta),\\
\sigma_{r\theta}(r, \theta) &= -Kr^{\lambda-1}\lambda f'(\theta),
\end{aligned} \tag{2-6}$$

where $\lambda - 1$ denotes the exponent representing the singularity of the stress field, and will be called the stress singularity exponent hereafter. According to (2-3), the asymptotic strain field as r tends to 0 takes the form $\varepsilon_{ij}(r, \theta) = K^n r^{(\lambda-1)n}\tilde{\varepsilon}_{ij}(\theta)$, or, in expanded form,

$$\begin{aligned}
\varepsilon_{rr}(r, \theta) &= \tfrac{1}{2}BK^n r^{(\lambda-1)n} f_e^{n-1}[(\lambda+1)(2-\lambda)f(\theta) + 2f''(\theta)],\\
\varepsilon_{\theta\theta}(r, \theta) &= \tfrac{1}{2}BK^n r^{(\lambda-1)n} f_e^{n-1}[(\lambda+1)(2\lambda-1)f(\theta) - f''(\theta)],\\
\varepsilon_{r\theta}(r, \theta) &= -\tfrac{3}{2}BK^n r^{(\lambda-1)n} f_e^{n-1}\lambda f'(\theta).
\end{aligned}$$

The compatibility condition (2-2) results in the following nonlinear fourth-order ODE for $f(\theta)$:

$$
\begin{aligned}
0 = {} & f^{\mathrm{IV}} f_e^2\{(n-1)\big[(\lambda+1)(2-\lambda)f+2f''\big]^2+2f_e^2\}\\
& +6[(\lambda)n+1]\lambda\big[(n-1)f_e^2hf'+f_e^4f''\big]+(n-1)(n-3)h^2\big[(\lambda+1)(2-\lambda)f+2f''\big]\\
& +(n-1)f_e^2\big[(\lambda+1)(2-\lambda)f+2f''\big]\\
& \quad\times\Big\{\big[(\lambda+1)f'+f'''\big]^2+\big[(\lambda+1)f+f''\big](\lambda+1)f''+(\lambda+1)^2\lambda^2(f'^2+ff'')\\
& \qquad -\tfrac{1}{2}(\lambda+1)^2\lambda ff''-\big[(\lambda+1)f'+f'''\big](\lambda+1)\lambda f'\\
& \qquad -\tfrac{1}{2}\big[(\lambda+1)f+f''\big](\lambda+1)\lambda f''+3\lambda^2(f''^2+f'f''')\Big\}\\
& +f_e^4(\lambda+1)(2-\lambda)f''-(\lambda-1)nf_e^4\big[(\lambda+1)(2-\lambda)f+2f''\big]\\
& +[(\lambda-1)n+1](\lambda-1)nf_e^4\big[(\lambda+1)(2\lambda-1)f-f''\big]+2(n-1)f_e^2h\big[(\lambda+1)(2-\lambda)f'+2f''\big], \qquad (2\text{-}7)
\end{aligned}
$$

where we have adopted the notation

$$
\begin{aligned}
f_e &= \sqrt{\big[(\lambda+1)f+f''\big]^2+(\lambda+1)^2\lambda^2f^2-\big[(\lambda+1)f+f''\big](\lambda+1)\lambda f+3\lambda^2f'^2},\\
h &= \big[(\lambda+1)f+f''\big]\big[(\lambda+1)f'+f'''\big]+(\lambda+1)^2\lambda^2ff'-\tfrac{1}{2}\big[(\lambda+1)f'+f'''\big](\lambda+1)\lambda f\\
&\quad -\tfrac{1}{2}\big[(\lambda+1)f+f''\big](\lambda+1)\lambda f'+3\lambda^2f'f''.
\end{aligned}
$$

The boundary conditions imposed on the function $f(\theta)$ follow from the traction-free boundary conditions on the crack surfaces:

$$
f(\theta=\pm\pi)=0, \quad f'(\theta=\pm\pi)=0. \qquad (2\text{-}8)
$$

Thus, the eigenfunction expansion method results in a nonlinear eigenvalue problem: it is necessary to find eigenvalues λ leading to nontrivial solutions of (2-7) satisfying the boundary conditions (2-8). Therefore, the order of the stress singularity is the eigenvalue and the angular variations of the field quantities correspond to the eigenfunctions. When we consider mode I loading or mode II loading conditions, the symmetry or antisymmetry requirements of the problem with respect to the crack plane at $\theta=0$ are utilized. Due to the symmetry (or antisymmetry), the solution is sought for one of the half-planes, for instance, $0\le\theta\le\pi$. In analyzing the crack problem under mixed-mode loading conditions, the symmetry or antisymmetry arguments cannot be used, and it is necessary to seek the solution in the whole plane $-\pi\le\theta\le\pi$. To find the numerical solution, one has to take into account the value of the mixity parameter M^p characterizing the mixities of mode I and mode II loadings. For this purpose, in the framework of the proposed technique, (2-7) is numerically solved on the interval $[0,\pi]$, and the two-point boundary value problem is reduced to the initial value problem with the initial conditions reflecting the value of the mixity parameter:

$$
f(\theta=0)=1, \quad f'(\theta=0)=(\lambda+1)/\tan\big(\tfrac{1}{2}M^p\pi\big), \quad f(\theta=\pi)=0, \quad f'(\theta=\pi)=0. \qquad (2\text{-}9)
$$

The first initial condition is the normalization condition. The second condition follows from (2-4) specifying the value of the mixity parameter. At the next stage, the numerical solution of (2-7) is found on the interval $[-\pi,0]$, with the following boundary conditions which have to be satisfied:

$$
f(\theta=-\pi)=0, \quad f'(\theta=-\pi)=0, \quad f(\theta=0)=1, \quad f'(\theta=0)=(\lambda+1)/\tan\big(\tfrac{1}{2}M^p\pi\big). \qquad (2\text{-}10)
$$

An analogous approach was adopted in [Stepanova and Adylina 2014], where the near mixed-mode crack-tip stress field under plane strain conditions was analyzed. It is assumed that the eigenvalue of the problem considered equals the eigenvalue of the classical HRR problem, $\lambda = n/(n+1)$; see [Hutchinson 1968b; 1968a; Rice and Rosengren 1968] for pure mode I and pure mode II conditions; [Rice 1967; 1968] for pure mode III conditions. However, it turns out that when we construct the numerical solution for the mixed-mode crack problem under plane stress conditions the radial stress component $\sigma_{rr}(r,\theta)$ at $\theta = 0$ has a discontinuity, whereas for the cases of pure mode I and pure mode II loadings, when $M^p = 1$ and $M^p = 0$ are valid, the radial stress component is continuous at $\theta = 0$. Numerical analysis carried out previously for mixed-mode crack problem under plane strain conditions leads to the continuous angular distributions of the radial stress component $\sigma_{rr}(r,\theta)$ at $\theta = 0$ [Shlyannikov and Kislova 2009; Shlyannikov 2012]. In order to obtain the asymptotic solution of the mixed-mode I/II crack problem under plane stress conditions and to analyze the behavior of the radial stress components, one can use the artificial small parameter method often used for the solution of nonlinear eigenvalue problems [Andrianov and Awrejcewicz 2013; Andrianov et al. 2014; Nayfeh 2000; 2011].

3. Nonlinear eigenvalue problem. Perturbation theory method.

One of the effective methods for the solution of nonlinear eigenvalue problems is the perturbation theory technique based on an artificially introduced small parameter [Andrianov and Awrejcewicz 2013; Andrianov et al. 2014; Nayfeh 2000; 2011; Sliva et al. 2010]. An analytical expression for the eigenvalues of the nonlinear eigenvalue problem (2-7)–(2-8) can be derived by applying the perturbation theory method. For this purpose, the eigenvalue λ is split up into $\varepsilon = \lambda - \lambda_0$, where λ_0 refers to the "undisturbed" linear problem and ε is the deviation on account of the nonlinearity. Furthermore, the hardening exponent n and the stress function $f(\theta)$ are represented as power series:

$$\lambda = \lambda_0 + \varepsilon, \quad f(\theta) = f_0(\theta) + \varepsilon f_1(\theta) + \varepsilon^2 f_2(\theta) + \ldots, \quad n = 1 + \varepsilon n_1 + \varepsilon^2 n_2 + \ldots, \tag{3-1}$$

where $f_0(\theta)$ refers to the solution of the linear problem. Introducing (3-1) into (2-7), grouping together the terms with the same powers of ε and equating to zero, the set of the boundary value problems for $f_k(\theta)$ is obtained.

By equating the coefficients of ε^0, we obtain

$$\begin{gathered} f_0^{\mathrm{IV}} + 2(\lambda_0^2+1) f_0'' + (\lambda_0^2-1)^2 f_0 = 0, \\ f_0(\theta=0) = 1, \quad f_0'(\theta=0) = (\lambda_0+1)/\tan\left(\tfrac{1}{2}M^p\pi\right), \quad f_0(\theta=\pi), \quad f_0'(\theta=\pi), \\ f_0(\theta=-\pi), \quad f_0'(\theta=-\pi), \quad f_0(\theta=0) = 1, \quad f_0'(\theta=0) = (\lambda_0+1)/\tan\left(\tfrac{1}{2}M^p\pi\right); \end{gathered} \tag{3-2}$$

by equating the coefficients of ε^1, we obtain

$$\begin{gathered} f_1^{\mathrm{IV}} + 2(\lambda_0^2+1) f_1'' + (\lambda_0^2-1)^2 f_1 = -n_1\left[x_0(f_0^{\mathrm{IV}} x_0/2 + w_0)/(2g_0) + h_0(x_0' g_0 - x_0 h_0 + 3\lambda_0^2 g_0 f_0')/g_0^2\right] \\ -\tfrac{1}{2} f_0''\left[(\lambda_0-1)(4\lambda_0-1)n_1 + 8\lambda_0\right] - \tfrac{1}{2} f_0(\lambda_0^2-1)\left[(\lambda_0-1)(4\lambda_0+1)n_1 + 8\lambda_0\right], \\ f_1(\theta=0) = 0, \quad f_1'(\theta=0) = 1/\tan\left(\tfrac{1}{2}M^p\pi\right), \quad f_1(\theta=\pi), \quad f_1'(\theta=\pi), \\ f_1(\theta=-\pi), \quad f_1'(\theta=-\pi), \quad f_1(\theta=0) = 0, \quad f_1'(\theta=0) = 1/\tan\left(\tfrac{1}{2}M^p\pi\right); \end{gathered} \tag{3-3}$$

by equating the coefficients of ε^2, we obtain

$$
\begin{aligned}
&f_2^{\mathrm{IV}} + 2(\lambda_0^2+1)f_2'' + (\lambda_0^2-1)^2 f_2 = -2g_1\big[f_1^{\mathrm{IV}} + 2(\lambda_0^2+1)f_1'' + (\lambda_0^2-1)^2 f_1\big]/g_0\\
&\quad - 3\lambda_0[2+n_1(\lambda_0-1)]f_1'' - \tfrac{1}{2}(1-2\lambda_0)\big[f_1'' + (\lambda_0-1)f_1\big] + \tfrac{1}{2}[1+n_1(\lambda_0-1)]x_1\\
&\quad - \tfrac{1}{2}\lambda_0(\lambda_0-1)(4\lambda_0+1)f_1 + \tfrac{1}{2}(1-2\lambda_0)[1+n_1(\lambda_0-1)]y_1\\
&\quad - 3\lambda_0[n_1+n_2(\lambda_0-1)]f_1'' - 3[1+n_1(\lambda_0-1)]f_0'' + \tfrac{1}{2}f_0'' - \tfrac{1}{2}(\lambda_0-1)f_0\\
&\quad + \tfrac{1}{2}[1+n_1(\lambda_0-1)](1-2\lambda_0)\big[f_0 + (4\lambda_0+1)f_0\big] - \lambda_0(\lambda_0-1)f_0\\
&\quad - \tfrac{1}{2}(2\lambda_0-1)[n_1+n_2(\lambda_0-1)]y_0 - \tfrac{1}{2}[1+n_1(\lambda_0-1)]^2 y_0 + \tfrac{1}{2}[n_1+n_2(\lambda_0-1)]x_0\\
&\quad - g_1\big\{6\lambda_0[2+n_1(\lambda_0-1)]f_0'' + (1-2\lambda_0)\big[f_0'' - (\lambda_0-1)f_0\big] - [1+n_1(\lambda_0-1)]x_0\big\}/g_0\\
&\quad - g_1\big\{\lambda_0(\lambda_0-1)(4\lambda_0+1)f_0 + (2\lambda_0-1)[1+n_1(\lambda_0-1)]y_0\big\}/g_0\\
&\quad - n_2\big\{x_0\big(f_0^{\mathrm{IV}}x_0/2 + w_0\big)/(2g_0) + h_0\big(g_0x_0' - x_0h_0 + 3\lambda_0^2 g_0 f_0'\big)/g_0^2\big\}\\
&\quad - n_1\big[x_0g_0(f_1^{\mathrm{IV}}x_0/2 + w_1) + x_0g_1(f_0^{\mathrm{IV}}x_0/2 + w_0) + g_0x_1(f_0^{\mathrm{IV}}x_0 + w_0)\big]/(2g_0^2)\\
&\quad - n_1\big\{h_0[x_1'g_0 - x_1h_0 + 3\lambda_0^2 g_0 f_1'] + h_0[x_0'g_1 - x_0h_1 + 3\lambda_0^2 g_1 f_0']\big\}/g_0^2\\
&\quad - n_1\big\{6\lambda_0[2+n_1(\lambda_0-1)]g_0h_0f_0' - (1-2\lambda_0)\big[2h_0^2f_0 - 2g_0h_0f_0'\big] + n_1h_0^2x_0\big\}/(2g_0^2)\\
&\quad - n_1(1-2\lambda_0)f_0(f_0^{\mathrm{IV}}x_0 + w_0)/(2g_0) - n_1h_1\big(x_0'g_0 - x_0h_0 + 3\lambda_0^2g_0f_0'\big)/g_0^2;\\
&\qquad f_2(\theta=0)=0, \quad f_2'(\theta=0) = 1/\tan\big(\tfrac{1}{2}M^p\pi\big), \quad f_2(\theta=\pi), \quad f_2'(\theta=\pi),\\
&\quad f_2(\theta=-\pi), \quad f_2'(\theta=-\pi), \quad f_2(\theta=0)=0, \quad f_2'(\theta=0) = 1/\tan\big(\tfrac{1}{2}M^p\pi\big),
\end{aligned}
\tag{3-4}
$$

where we have adopted the notation

$$
\begin{aligned}
&x_k = (\lambda_0+1)(2-\lambda_0)f_k + 2f_k'', \quad y_k = (\lambda_0+1)(2\lambda_0-1)f_k - f_k'', \quad u_k = (\lambda_0+1)f_k + f_k'',\\
&v_k = (\lambda_0+1)\lambda_0 f_k, \quad g_0 = u_0^2 + v_0^2 - u_0v_0 + 3\lambda_0^2 f_0'^2,\\
&h_0 = u_0u_0' + v_0v_0' - \tfrac{1}{2}u_0'v_0 - \tfrac{1}{2}u_0v_0' + 3\lambda_0^2 f_0'f_0'',\\
&w_0 = u_0'^2 + (\lambda_0+1)u_0f_0'' + v_0'^2 + v_0v_0'' - \tfrac{1}{2}(\lambda_0+1)v_0f_0'' - u_0v_0' - \tfrac{1}{2}u_0v_0'' + 3\lambda_0^2(f_0''^2 + f_0'f_0'''),\\
&g_1 = 2u_0(u_1+f_0) + 2v_0\big[v_1 + (2\lambda+1)f_0\big] - u_0\big[v_1 + (2\lambda+1)f_0\big] - v_0(u_1+f_0)\\
&\qquad + 6\lambda_0 f_0'(\lambda_0 f_1' + f_0'),\\
&h_1 = u_0(u_1' + f_0') + u_0'(u_1+f_0) + v_0\big[v_1' + (2\lambda_0+1)f_0'\big] + v_0'\big[v_1 + (2\lambda_0+1)f_0\big]\\
&\qquad - \tfrac{1}{2}u_0'\big[v_1 + (2\lambda_0+1)f_0\big] - \tfrac{1}{2}u_0\big[v_1' + (2\lambda_0+1)f_0'\big] - \tfrac{1}{2}v_0(u_1' + f_0') - \tfrac{1}{2}v_0'(u_1+f_0)\\
&\qquad + 3\lambda_0 f_0'(\lambda_0 f_1'' + f_0'') + 3\lambda_0 f_0''(\lambda_0 f_1' + f_0'),\\
&w_1 = 2u_0'(u_1' + f_0') + u_0\big[(\lambda_0+1)f_1'' + f_0''\big] + (\lambda_0+1)f_0''(u_1+f_0) + 2v_0'\big[v_1' + (2\lambda_0+1)f_0'\big]\\
&\qquad + v_0'\big[v_1'' + (2\lambda_0+1)f_0''\big] + v_0''\big[v_1 + (2\lambda_0+1)f_0\big] - \tfrac{1}{2}(\lambda_0+1)f_0''\big[v_1 + (2\lambda_0+1)f_0\big]\\
&\qquad - \tfrac{1}{2}v_0\big[(\lambda_0+1)f_1'' + f_0''\big] - v_0'(u_1' + f_0') - u_0'\big[v_1' + (2\lambda_0+1)f_0'\big] - \tfrac{1}{2}v_0''(u_1+f_0)\\
&\qquad - \tfrac{1}{2}u_0\big[v_1'' + (2\lambda_0+1)f_0''\big] + 6\lambda_0 f_0''(\lambda_0 f_1'' + f_0'') + 3\lambda_0 f_0'''(\lambda_0 f_1' + f_0') + 3\lambda_0 f_0'(\lambda_0 f_1''' + f_0''').
\end{aligned}
$$

The solution of the linear ordinary differential equation (3-2) for the function $f_0(\theta)$ satisfying the traction-free boundary conditions has the form

$$f_0^{\mathrm{I}} = \beta\cos(\alpha\theta) - \alpha\cos(\beta\theta), \quad \alpha = \lambda_0 - 1, \quad \beta = \lambda_0 + 1,$$

for the crack opening mode I (for symmetric stress fields), and it has the form

$$f_0^{\mathrm{II}} = \sin(\alpha\theta) - \sin(\beta\theta)$$

for the shear crack mode II (the skew-symmetric stress fields), where the spectrum of the eigenvalues is determined by the characteristic equation $\sin 2\pi\lambda_0 = 0$, whence one can easily find $\lambda_0 = \frac{1}{2}m$, where m is an integer. Thus it is shown that an infinite number of eigenvalues exists. In view of the linearity of (3-2) for the mixed-mode crack problem, the solution is the superposition of the symmetric and antisymmetric parts of the stress field with respect to the crack plane:

$$f_0(\theta) = C_1[\beta\cos(\alpha\theta) - \alpha\cos(\beta\theta)] + C_2[\sin(\alpha\theta) - \sin(\beta\theta)], \tag{3-5}$$

where C_1 and C_2 are unknown coefficients which have to be determined from the boundary conditions of the actual crack problem and represent the modes I and II, respectively. In view of (2-4), the unknown constants C_1 and C_2 are related to the mixity parameter $M^p = 2\arctan[(\lambda_0+1)C_1/C_2]/\pi$. The zeroth-order problem (3-2) has the nontrivial solution (3-5), hence the inhomogeneous problems (3-3), (3-4) for the functions $f_1(\theta)$ and $f_2(\theta)$ will not have solutions unless a solvability condition is satisfied [Nayfeh 2000; 2011]. Therefore, if λ_0 is not an eigenvalue of the homogeneous problem (i.e., the homogeneous problem has only the trivial solution), the inhomogeneous problem has a unique solution for every continuous right-hand side $G_k(\theta)$ of the differential equation for $f_k(\theta)$, $k > 0$. On the other hand, if λ_0 is an eigenvalue of the homogeneous problem (i.e., the homogeneous problem has a nontrivial solution), the inhomogeneous problem does not have a solution unless [Nayfeh 2000; 2011]

$$\int_{-\pi}^{\pi} G_k(\theta)u(\theta)\,d\theta = 0. \tag{3-6}$$

That is, $G_k(\theta)$ is orthogonal to the eigenfunction $u(\theta)$, corresponding to the eigenvalue λ_0. These results constitute the so-called Fredholm alternative theorem: for a given value λ_0, either the inhomogeneous problem has a unique solution for each continuous right-hand side of the equation, or else the homogeneous problem has a nontrivial solution [Nayfeh 2000; 2011]. To determine the solvability condition (3-6) we use the concept of adjoint problems [Stepanova 2008a; 2008b; 2009a; Stepanova and Igonin 2014]. The boundary value problem (3-3) is self-adjoint since the differential equation and the boundary conditions of the adjoint problem coincide with the differential equation and boundary conditions of the homogeneous problem (3-2). Therefore, $u(\theta) = f_0(\theta)$, where the function $f_0(\theta)$ is determined by (3-5). According to (3-6), the compatibility condition of the boundary value problem (3-3) has the form $\int_{-\pi}^{\pi} G_1(\theta)\,f_0(\theta)\,d\theta = 0$, or, in expanded form,

$$\begin{aligned}\int_{-\pi}^{\pi} \big\{ &-n_1[x_0(\tfrac{1}{2}f_0^{\mathrm{IV}}x_0 + w_0)/(2g_0) + h_0(g_0x_0' - x_0h_0 + 3\lambda_0^2 g_0 f_0')/g_0^2] \\ &- \tfrac{1}{2}f_0''[(\lambda_0-1)(4\lambda_0-1)n_1 + 8\lambda_0] - \tfrac{1}{2}f_0(\lambda_0^2-1)[(\lambda_0-1)(4\lambda_0+1)n_1 + 8\lambda_0]\big\} f_0(\theta)\,d\theta = 0.\end{aligned} \tag{3-7}$$

M^p	n_1	n_2	M^p	n_1	n_2	M^p	n_1	n_2
0	4.000000	8.000000	0.3	4.065772	7.941876	0.8	4.224060	7.926086
0.05	4.001766	7.999995	0.4	4.118594	7.804045	0.9	4.084774	7.958755
0.1	4.007088	7.999954	0.5	4.184135	7.749316	0.95	4.023759	7.999543
0.2	4.028722	7.978646	0.6	4.249098	7.600224	1	4.000000	8.000000
			0.7	4.279336	7.577773			

Table 1. Coefficients of the asymptotic expansion of the hardening exponent n.

The compatibility condition of the boundary value problem for the function $f_1(\theta)$ (3-7) allows us to find the coefficient n_1. The values of n_1 for different values of the mixity parameter are shown in Table 1. Having obtained the function $f_1(\theta)$, one can determine the unknown function $f_2(\theta)$. Using the analogous reasoning, one can formulate the compatibility condition for the solution of the boundary value problem for $f_2(\theta)$ and calculate numerically the values of the coefficient n_2 of the asymptotic expansion of the hardening exponent n for different values of the mixity parameter. Table 1 summarizes the results of computations and gives the coefficients n_1 and n_2 for different values of the mixity parameter.

From the results obtained one can see that the mixed-mode loading leads to change of the stress singularity in the vicinity of the crack tip under plane stress conditions. Previously, it was found [Stepanova 2008a; 2009a] that for mode I and mode II crack problems the perturbation theory technique results in the equation $n_k = (-1)^{k+1}/(\lambda_0 - 1)^{k+1}$ (where, for the HRR problem, $\lambda_0 = \frac{1}{2}$), and the third asymptotic expansion in (3-1) yields $n = \lambda/(1-\lambda)$, or $\lambda = n/(n+1)$. This eigenvalue corresponds to the classical HRR stress field. The results obtained and given in Table 1 clearly show that the mixed-mode loading leads to a change in the stress singularity exponent in the vicinity of the crack tip. Otherwise, the values of the coefficients n_1 and n_2 were 4 and 8, respectively, as they were in the case of plane strain conditions. In other words, if the coefficients n_1 and n_2 were equal to 4 and 8, respectively, then we would have $n_k = (-1)^{k+1}/(\lambda_0 - 1)^{k+1}$, [Stepanova 2008a; 2009a] and we would sum the binomial series for n and obtain the classical HRR stress field. However, as is indicated by Table 1, the values of n_1 and n_2 deviate from 4 and 8, respectively. Thus, mixed-mode loading causes a change in the stress singularity in the neighborhood of the crack tip. When we analyze the stress-strain state in the vicinity of the crack tip under mixed-mode loading, it is assumed that the stress singularity does not change and the eigenvalue corresponds to the HRR problem, $\lambda = n/(n+1)$ (i.e., it is assumed a priori that the eigenvalue equals $\lambda = n/(n+1)$ and the hypothesis is confirmed by the solution [Shlyannikov and Kislova 2009]). However, in the case of plane stress conditions, as the artificial small parameter method shows, the hypothesis cannot be accepted and it is necessary to find the eigenvalues of the problem as a part of the solution. In the next part of the paper, the numerical solution of the nonlinear eigenvalue problem will be considered.

4. Numerical solution of the nonlinear eigenvalue problem. Computational scheme. Eigenvalues and eigenfunctions.

As mentioned earlier, traditionally, it is assumed that the eigenvalue of the nonlinear eigenvalue problem equals the eigenvalue of the HRR problem: $\lambda = n/(n+1)$. However, the assumption results in the discontinuity of the radial stress component on the line extending the crack. The asymptotic analysis

based on the artificial small parameter method and described above has shown additionally that the eigenvalue corresponding to the HRR stress field cannot be the eigenvalue of the mixed-mode crack problem under plane stress conditions. In view of the above arguments, the eigenvalue of the problem considered will be determined from the requirement of the continuity of the radial stress component at $\theta = 0$. The analogous approach for solving the nonlinear eigenvalue problems has been applied in [Stepanova and Adylina 2014], where the approach allowed the determination of the whole spectrum of the eigenvalues, resulting in the contours of the completely damaged zone converging to the limit contour. The procedure of the numerical solution of the nonlinear eigenvalue problem is based on the following assumptions. In the case of the mixed-mode crack problem the symmetry and antisymmetry arguments cannot be used, and it is necessary to find the solution on the interval $[-\pi, \pi]$. In conducting the numerical solution, the interval $[-\pi, \pi]$ can be divided into two intervals: $[0, \pi]$ and $[-\pi, 0]$. First, (2-7) is numerically solved in the interval $[0, \pi]$, and the two-point boundary value problem (2-7), (2-9) is reduced to the initial problem with the initial conditions

$$f(\theta = 0) = 1, \quad f'(\theta = 0) = (\lambda + 1)/\tan\left(\tfrac{1}{2} M^p \pi\right), \quad f''(\theta = 0) = A_2, \quad f'''(\theta = 0) = A_3. \tag{4-1}$$

The unknown constants A_2 and A_3 are determined such that the boundary conditions on the upper crack surface are satisfied:

$$f(\theta = \pi) = 0, \quad f'(\theta = \pi) = 0. \tag{4-2}$$

The constants A_2 and A_3 having been obtained, (2-7) is numerically solved on the interval $[-\pi, 0]$. For this purpose, the two-point boundary value problem is reduced to the initial problem with the initial conditions

$$f(\theta = -\pi) = 0, \quad f'(\theta = -\pi) = 0, \quad f''(\theta = -\pi) = B_2, \quad f'''(\theta = -\pi) = B_3. \tag{4-3}$$

The unknown constants B_2 and B_3 are chosen in such a way that the equilibrium equations of the element belonging to the line $\theta = 0$ are satisfied. The equilibrium equations require the continuity of the shear and circumferential stress components $\sigma_{r\theta}(r, \theta)$ and $\sigma_{\theta\theta}(r, \theta)$ at $\theta = 0$, which implies the continuity of the functions $f(\theta)$ and $f'(\theta)$ at $\theta = 0$ (and, therefore, the boundary conditions (2-10), and hence discontinuities of the radial stress components are allowed). Thus, the two unknown constants B_2 and B_3 are determined in such a way that the solution on the interval $[-\pi, 0]$ satisfies the boundary conditions at $\theta = 0$. When this algorithm is realized, it is usually supposed that the eigenvalue equals the eigenvalue of the HRR stress field. If it is necessary to find eigenvalues different from $\lambda = n/(n + 1)$, and, as a whole, the spectrum of the eigenvalues, then the question arises: which additional physical and (or) mathematical reasons need to be invoked for finding the eigenspectrum? If λ is a required value, then under integration of (2-7) in the interval $[0, \pi]$ one has the three unknown parameters λ, A_2 and A_3, and only the two boundary conditions (4-2) from which the unknowns can be obtained. Obviously, it is necessary to have an additional condition. For the purpose of determination of the eigenvalue λ one can analyze the behavior of the radial stress component in the case of plane strain conditions [Shlyannikov and Kislova 2009; Stepanova and Adylina 2014]. One can see that the radial stress component is continuous as a function of the polar angle at $\theta = 0$ for the values of the mixity parameter and the hardening exponent. It should be noted that the continuity of the radial stress component is not a priori required (i.e., the eigenvalue corresponding to the HRR field $\lambda = n/(n + 1)$ has been chosen and the radial stress

M^p	λ	$f''(\theta=0)$	$f'''(\theta=0)$	$f''(\theta=-\pi)$	$f'''(\theta=-\pi)$
0.1	0.749848	−1.013963	−17.857405	−11.119908	0.112696
0.2	0.749363	−1.009899	−8.639267	−5.450935	0.210905
0.3	0.748445	−1.002588	−5.438885	−3.518917	0.244099
0.4	0.746893	−0.991172	−3.732943	−2.521575	0.262339
0.5	0.744332	−0.974435	−2.613062	−1.898950	0.276300
0.6	0.740101	−0.951096	−1.774144	−1.465507	0.290927
0.7	0.733089	−0.921053	−1.087827	−1.143866	0.311439
0.8	0.721666	−0.889149	−0.501650	−0.898579	0.348145
0.9	0.710960	−0.878015	−0.059127	−0.724120	0.428064

Table 2. New eigenvalues λ for $n = 3$ for different values of the mixity parameter.

component $\sigma_{rr}(r, \theta)$ turned out to be continuous for all the values of the mixity parameter and for all the values of the hardening exponent). Therefore, the eigenvalue is sought from the requirement of the continuity of the radial stress component $\sigma_{rr}(r, \theta)$ at $\theta = 0$. Thus, the spectrum of the eigenvalues is numerically obtained.

The numerical integration of differential equation (2-7) to obtain $f(\theta)$ for $[0, \pi]$ is performed by the fourth-order Runge–Kutta method, using symbolic computation in Mathematica as a powerful, convenient and versatile tool widely used in solid mechanics [Constantinescu and Korsunsky 2007], while the solution of the simultaneous nonlinear equations

$$f(\pi) = F_1(A_2, A_3) = 0, \quad f'(\pi) = F_2(A_2, A_3) = 0$$

for A_2, A_3 for a prescribed value of λ is obtained by the Gauss–Newton least-square method so that they satisfy the condition $(f(\pi))^2 + (f'(\pi))^2 < 10^{-7}$. Next the solution is sought for the interval $[-\pi, 0]$ and the numerical integration of (2-7) is performed by the fourth-order Runge–Kutta method whereas the solution of simultaneous nonlinear equations

$$f(-\pi) = F_3(B_2, B_3) = 0, \quad f'(-\pi) = F_4(B_2, B_3) = 0$$

for B_2, B_3 for the same prescribed value of λ is obtained by Gauss–Newton least-square method so that they satisfy the condition $(f(-\pi))^2 + (f'(-\pi))^2 < 10^{-7}$. Then one can compare the values of the radial stress component at $\theta = 0$: $\tilde{\sigma}_{rr}(\theta = 0^-)$ and $\tilde{\sigma}_{rr}(\theta = 0^+)$. The eigenvalue λ is said to be found if the inequality $|(\tilde{\sigma}_{rr}(\theta = 0^+) - \tilde{\sigma}_{rr}(\theta = 0^-)| < 10^{-7}$ is valid.

Results of computations are shown in Tables 2–7, where the new eigenvalues λ and the values of the functions $f''(\theta = 0)$, $f'''(\theta = 0)$, $f''(\theta = -\pi)$ and $f'''(\theta = -\pi)$ for the different values of the mixity parameter M^p and the hardening exponent n are given.

Circumferential variations of the stress and strain components obtained are shown in Figures 1–8. The contours of the equal equivalent stress are shown in Figure 9. It is shown that the angular stress distributions are fully continuous and do not contain the discontinuities.

In [Ondraček and Materna 2014], FEM evaluation of the dissipated energy in front of a crack tip under 2D mixed-mode loading conditions was performed. Two different meshes were created to simulate mode I and mode II fatigue crack growth. In both cases, the plane stress and strain calculations were

M^p	λ	$f''(\theta=0)$	$f'''(\theta=0)$	$f''(\theta=-\pi)$	$f'''(\theta=-\pi)$
0.1	0.833249	−1.059014	−17.175345	−12.817403	0.217377
0.2	0.832975	−1.054353	−8.270256	−6.295063	0.214040
0.3	0.832434	−1.045751	−5.310084	−4.075287	0.211815
0.4	0.831456	−1.031834	−3.692485	−2.931140	0.210848
0.5	0.829711	−1.010626	−2.474608	−2.217574	0.211543
0.6	0.826595	−0.980308	−1.877300	−1.720923	0.214889
0.7	0.821183	−0.942182	−0.945119	−1.353750	0.223389
0.8	0.813522	−0.910480	−0.379570	−1.085758	0.244019
0.9	0.813057	−0.918935	−0.078809	−0.934756	0.294866

Table 3. New eigenvalues λ for $n = 5$ for different values of the mixity parameter.

M^p	λ	$f''(\theta=0)$	$f'''(\theta=0)$	$f''(\theta=-\pi)$	$f'''(\theta=-\pi)$
0.1	0.874951	−1.068014	−16.399514	−14.051259	0.275592
0.2	0.874787	−1.063523	−8.019713	−6.907737	0.218081
0.3	0.874448	−1.054980	−5.004927	−4.477821	0.197231
0.4	0.873779	−1.040530	−3.427356	−3.225923	0.186395
0.5	0.872529	−1.017364	−2.369760	−2.444916	0.180489
0.6	0.870107	−0.983152	−1.789715	−1.900363	0.178418
0.7	0.865837	−0.941813	−0.850487	−1.498387	0.181311
0.8	0.863118	−0.931654	−0.409135	−1.230020	0.194901
0.9	0.863005	−0.939455	−0.117494	−1.070440	0.230710

Table 4. New eigenvalues λ for $n = 7$ for different values of the mixity parameter.

M^p	λ	$f''(\theta=0)$	$f'''(\theta=0)$	$f''(\theta=-\pi)$	$f'''(\theta=-\pi)$
0.1	0.899969	−1.067810	−15.870539	−14.973046	0.300772
0.2	0.899986	−1.063699	−7.757085	−7.364961	0.214921
0.3	0.899637	−1.055617	−4.929978	−4.777032	0.184458
0.4	0.899167	−1.041283	−3.428549	−3.445052	0.168585
0.5	0.898187	−1.017020	−2.446724	−2.613278	0.159358
0.6	0.896185	−0.979984	−1.473179	−2.032212	0.154562
0.7	0.892756	−0.938703	−0.786691	−1.605170	0.154589
0.8	0.892187	−0.945074	−0.441700	−1.335332	0.164138
0.9	0.892132	−0.951743	−0.148784	−1.166821	0.191437

Table 5. New eigenvalues λ for $n = 9$ for different values of the mixity parameter.

performed. The crack zones under conditions of plane stress are rather oval shaped. The shape of the equal equivalent stress contours shown in the first three rows of Figure 9 is similar to results of [Ondraček and Materna 2014].

M^p	λ	$f''(\theta=0)$	$f'''(\theta=0)$	$f''(\theta=-\pi)$	$f'''(\theta=-\pi)$
0.1	0.916646	−1.064886	−15.509504	−15.687120	0.308561
0.2	0.916575	−1.061186	−7.505140	−7.718823	0.207926
0.3	0.916414	−1.053681	−4.740118	−5.009507	0.172524
0.4	0.916060	−1.039712	−3.250966	−3.614202	0.154108
0.5	0.915260	−1.014674	−2.235656	−2.742892	0.143208
0.6	0.913531	−0.975351	−1.415360	−2.133091	0.137003
0.7	0.911361	−0.945900	−0.796175	−1.696655	0.135580
0.8	0.911145	−0.954022	−0.468121	−1.415250	0.142450
0.9	0.911123	−0.959920	−0.172574	−1.239380	0.164364

Table 6. New eigenvalues λ for $n = 11$ for different values of the mixity parameter.

M^p	λ	$f''(\theta=0)$	$f'''(\theta=0)$	$f''(\theta=-\pi)$	$f'''(\theta=-\pi)$
0.1	0.928557	−1.061240	−15.147594	−16.257399	0.307317
0.2	0.928507	−1.057923	−7.398140	−8.001191	0.199333
0.3	0.928389	−1.051006	−4.705468	−5.194292	0.161542
0.4	0.928110	−1.037485	−3.273920	−3.748906	0.141919
0.5	0.927433	−1.011819	−2.331595	−2.845877	0.130222
0.6	0.925895	−0.970589	−1.366626	−2.212890	0.123306
0.7	0.924700	−0.958252	−0.8289902	−1.777736	0.121104
0.75	0.924300	−0.965607	−0.634815	−1.606930	0.122390
0.8	0.924467	−0.960475	−0.489375	−1.478170	0.126133
0.9	0.924460	−0.965742	−0.190855	−1.295977	0.144355
0.95	0.924459	−0.967010	−0.044076	−1.245296	0.162210

Table 7. New eigenvalues λ for $n = 13$ for different values of the mixity parameter.

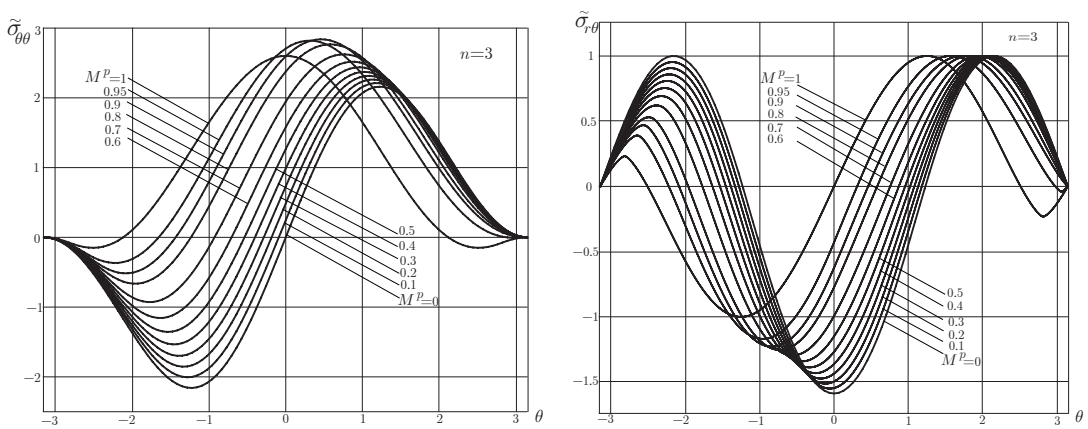

Figure 1. Circumferential variations of the stress components $\tilde{\sigma}_{\theta\theta}$ and $\tilde{\sigma}_{r\theta}$ for different values of the mixity parameter. Strain hardening exponent $n = 3$.

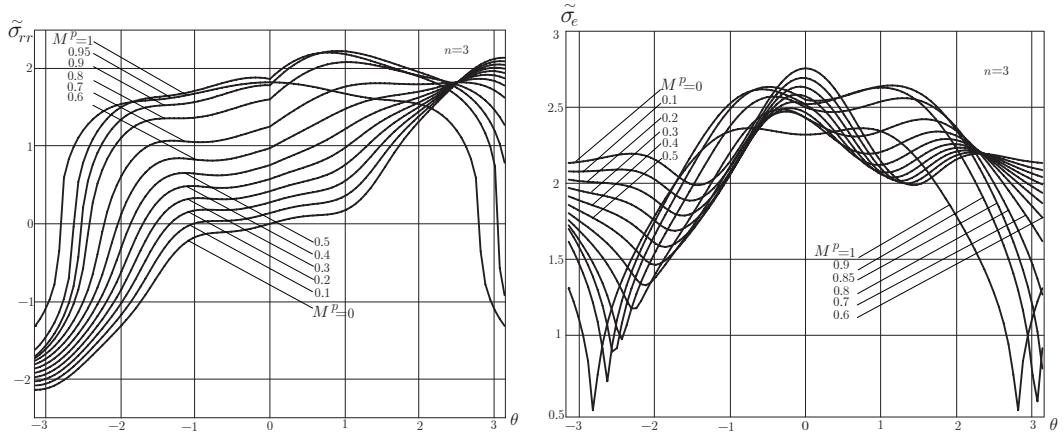

Figure 2. Circumferential variations of the stress component $\tilde{\sigma}_{rr}$ and the equivalent stress $\tilde{\sigma}_e$ for different values of the mixity parameter. Strain hardening exponent $n = 3$.

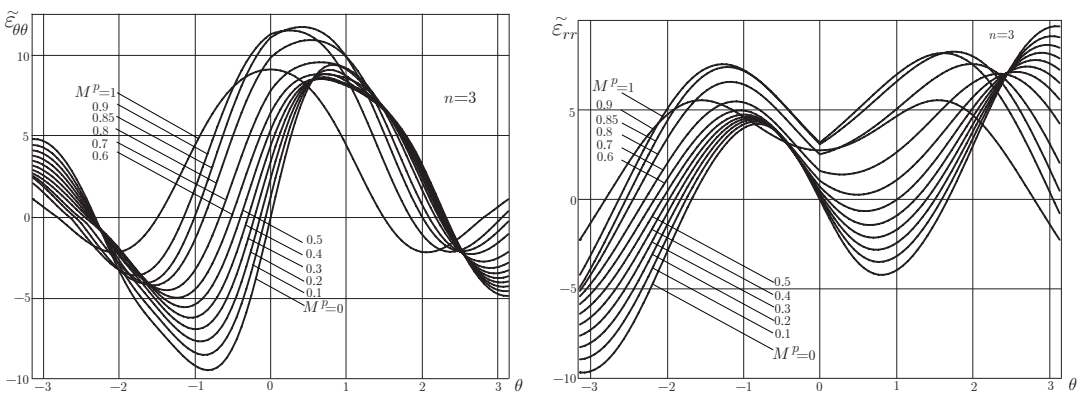

Figure 3. Circumferential variations of the strain components $\tilde{\varepsilon}_{\theta\theta}$ and $\tilde{\varepsilon}_{rr}$ for different values of the mixity parameter. Strain hardening exponent $n = 3$.

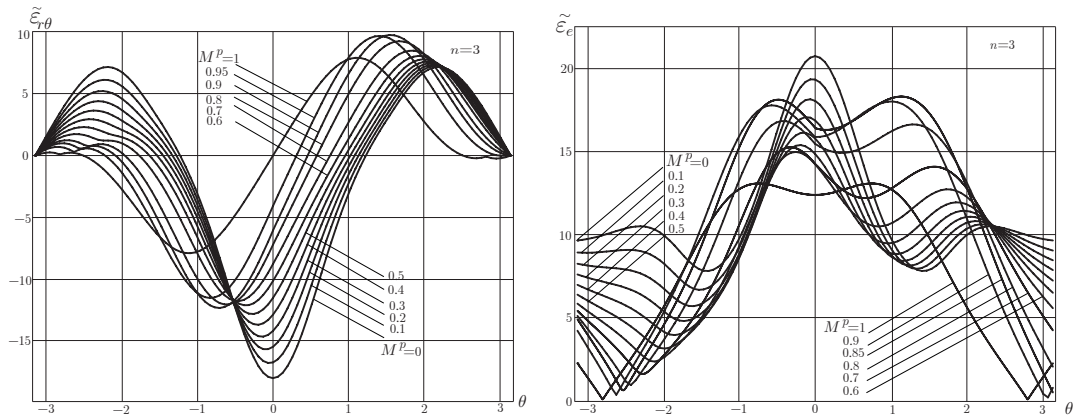

Figure 4. Circumferential variations of the strain component $\tilde{\varepsilon}_{r\theta}$ and the equivalent strain $\tilde{\varepsilon}_e$ for different values of the mixity parameter. Strain hardening exponent $n = 3$.

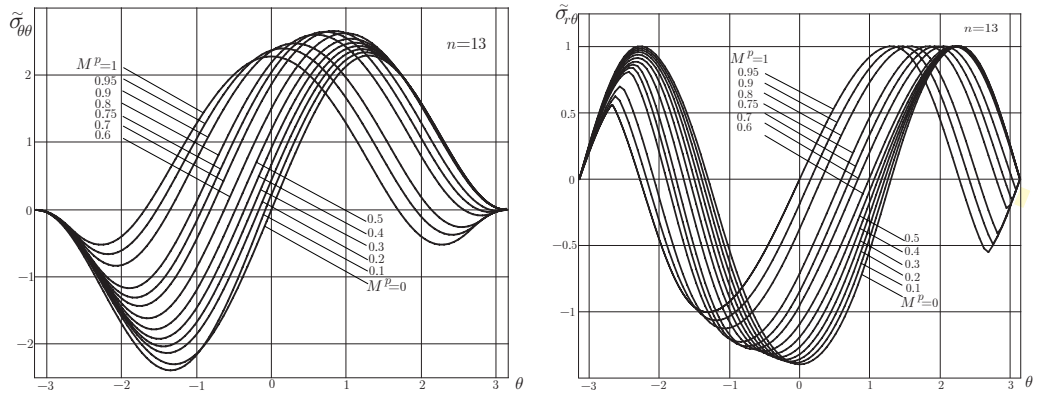

Figure 5. Circumferential variations of the stress components $\tilde{\sigma}_{\theta\theta}$ and $\tilde{\sigma}_{r\theta}$ for different values of the mixity parameter. Strain hardening exponent $n = 13$.

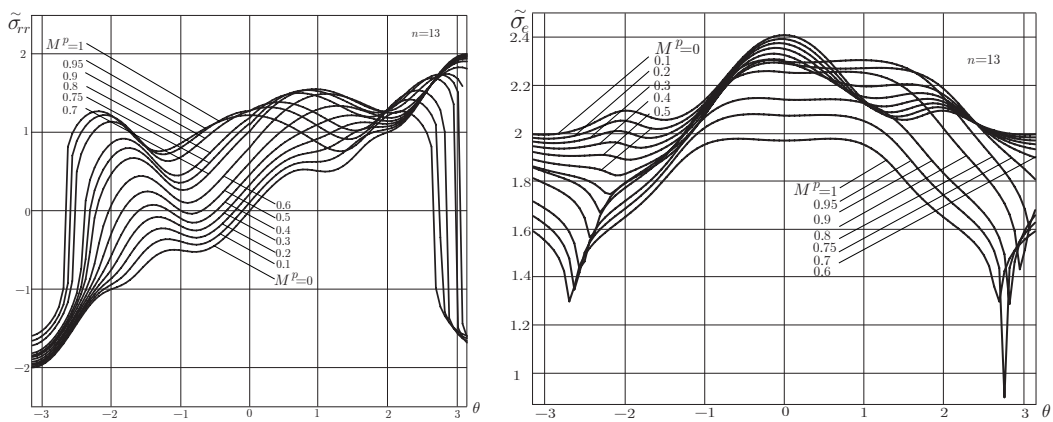

Figure 6. Circumferential variations of the stress component $\tilde{\sigma}_{rr}$ and the equivalent stress $\tilde{\sigma}_e$ for different values of the mixity parameter. Strain hardening exponent $n = 13$.

$M^p = 0.3$		$M^p = 0.5$		$M^p = 0.7$		$M^p = 0.8$	
n	δ, %	n	δ, %	n	δ, %	n	δ, %
3	0.207	3	0.75	3	2.25	3	3.77
5	0.107	5	0.43	5	1.45	5	2.37
7	0.063	7	0.28	7	1.04	7	1.35
9	0.040	9	0.20	9	0.80	9	0.86
11	0.027	11	0.15	11	0.57	11	0.60
13	0.019	13	0.12	13	0.41	13	0.44

Table 8. The difference between λ and λ_{HRR} for $M^p = 0.3, 0.5, 0.7, 0.8$.

One can evaluate the deviation of the new eigenvalue λ from the eigenvalue corresponding to the classical HRR stress field λ_{HRR}. The discrepancy $\delta = (\lambda_{\text{HRR}} - \lambda) * 100\%/\lambda_{\text{HRR}}$ for different values of the hardening exponent n and for different values of the mixity parameter M^p is given by Table 8.

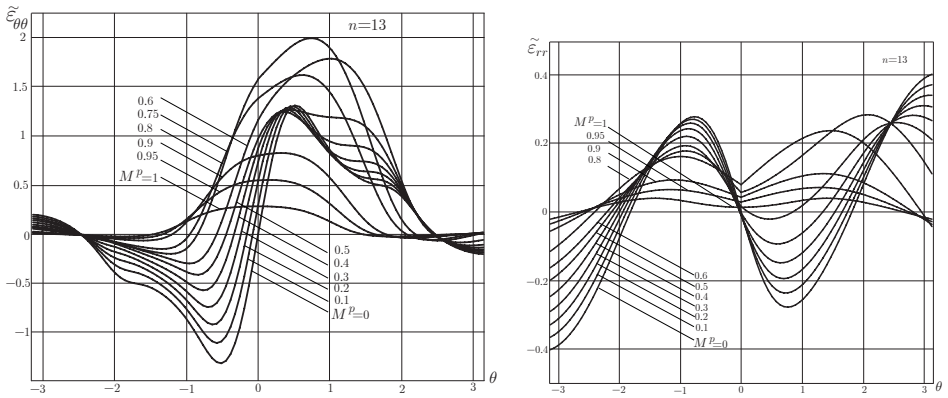

Figure 7. Circumferential variations of the strain components $\tilde{\varepsilon}_{\theta\theta}$ and $\tilde{\varepsilon}_{rr}$ for different values of the mixity parameter. Strain hardening exponent $n = 13$.

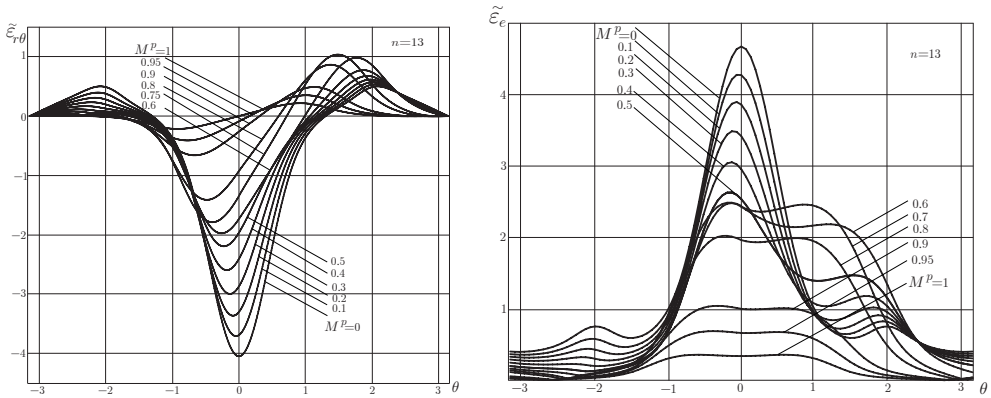

Figure 8. Circumferential variations of the strain component $\tilde{\varepsilon}_{r\theta}$ and the equivalent strain $\tilde{\varepsilon}_e$ for different values of the mixity parameter. Strain hardening exponent $n = 13$.

One can see from Table 8 that the difference tends to zero as the hardening exponent n increases, for all values of the mixity parameter. Thus, in the limiting case of perfect plasticity one can obtain the classical strain singularity r^{-1} and the vanishing singularity of the stress field in the vicinity of the crack tip. In the limiting case of perfect plasticity, the stresses should be bounded as $r \to 0$, and one can obtain the analytical solution of the problem in the asymptotic form

$$\sigma_{ij}(r,\theta) = \sigma_{ij}^{(0)}(\theta) + r^{\alpha}\sigma_{ij}^{(1)}(\theta) + \cdots, \quad \sigma_e(r,\theta) = 1 - r^{\alpha}\sigma^{(1)}(\theta) + \cdots, \quad \alpha > 0,\ r \to 0, \tag{4-4}$$

where the stresses are normalized by the yield stress. The governing system of equations following from the equilibrium equations and the Huber–Mises yield criterion can be found for functions $\sigma_{ij}^{(0)}(\theta)$:

$$\sigma_{r\theta,\theta}^{(0)} + \sigma_{rr}^{(0)} - \sigma_{\theta\theta}^{(0)} = 0, \quad \sigma_{\theta\theta,\theta}^{(0)} + 2\sigma_{r\theta}^{(0)} = 0, \quad (\sigma_{rr}^{(0)})^2 + (\sigma_{\theta\theta}^{(0)})^2 - \sigma_{rr}^{(0)}\sigma_{\theta\theta}^{(0)} + 3(\sigma_{r\theta}^{(0)})^2 = 1. \tag{4-5}$$

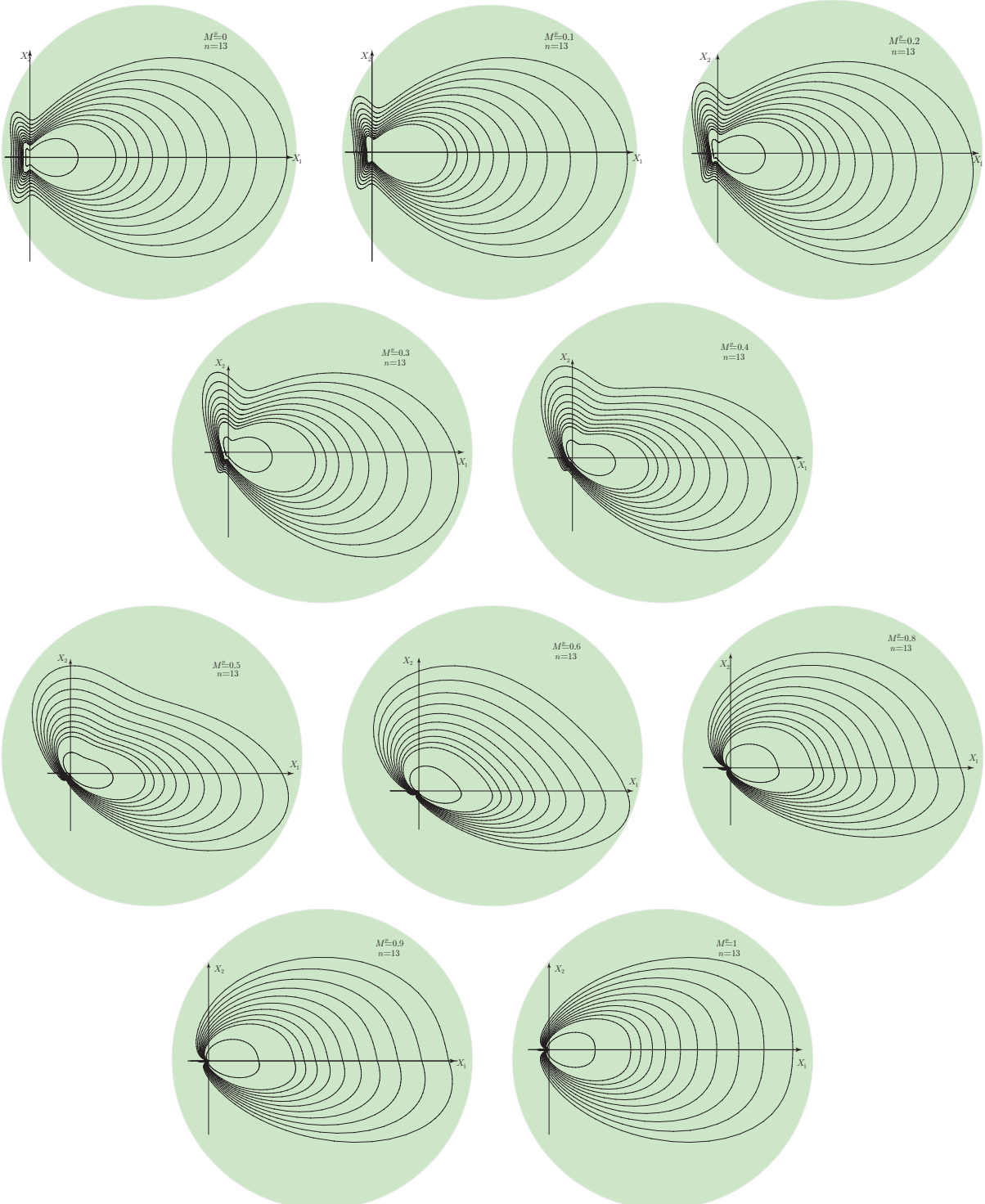

Figure 9. The contours of the equal equivalent stress $\sigma_e(r, \theta)$ in the vicinity of the crack tip.

The analytical expressions for the angular distributions $\sigma_{ij}^{(0)}(\theta)$ of the stress components for $M^p = 0.25$ are given as follows:

- For $-\pi \le \theta \le \theta_\alpha$, $\theta_\alpha = -2.186257912 = -125.26°$, we have

$$\sigma_{rr}^{(0)} = \tfrac{1}{2}(1+\cos 2\theta), \quad \sigma_{\theta\theta}^{(0)} = \tfrac{1}{2}(1-\cos 2\theta), \quad \sigma_{r\theta}^{(0)} = -\tfrac{1}{2}\sin 2\theta,$$

- For $\theta_\alpha \le \theta \le \theta_\beta$, $\theta_\beta = -1.686144171 = -96.60°$, we have

$$\sigma_{rr}^{(0)} = \tfrac{1}{\sqrt{3}}\cos(\theta+c_3), \quad \sigma_{\theta\theta}^{(0)} = \tfrac{2}{\sqrt{3}}\cos(\theta+c_3), \quad \sigma_{r\theta}^{(0)} = \tfrac{1}{\sqrt{3}}\sin(\theta+c_3),$$

  where $c_3 = 1.230959418 = 70.53°$.

- For $\theta_\beta \le \theta \le \theta_\gamma$, $\theta_\gamma = -0.9114267175 = -52.22°$, $\vartheta_1 = \theta_\beta + c_3$, we have

$$\sigma_{rr}^{(0)} = \tfrac{\sqrt{3}}{2}\cos\vartheta_1 - \tfrac{1}{2\sqrt{3}}\cos\vartheta_1\cos 2(\theta-\theta_\beta) + \tfrac{1}{\sqrt{3}}\sin\vartheta_1\sin 2(\theta-\theta_\beta),$$
$$\sigma_{\theta\theta}^{(0)} = \tfrac{\sqrt{3}}{2}\cos\vartheta_1 + \tfrac{1}{2\sqrt{3}}\cos\vartheta_1\cos 2(\theta-\theta_\beta) - \tfrac{1}{\sqrt{3}}\sin\vartheta_1\sin 2(\theta-\theta_\beta),$$
$$\sigma_{r\theta}^{(0)} = \tfrac{1}{2\sqrt{3}}\cos\vartheta_1\sin 2(\theta-\theta_\beta) + \tfrac{1}{\sqrt{3}}\sin\vartheta_1\cos 2(\theta-\theta_\beta).$$

- For $\theta_\gamma \le \theta \le \theta_\delta$, $\theta_\delta = 0.924219118 = 52.95°$, we have

$$\sigma_{rr}^{(0)} = \tfrac{1}{\sqrt{3}}\cos(\theta+c_1), \quad \sigma_{\theta\theta}^{(0)} = \tfrac{2}{\sqrt{3}}\cos(\theta+c_1), \quad \sigma_{r\theta}^{(0)} = \tfrac{1}{\sqrt{3}}\sin(\theta+c_1),$$

  where $c_1 = 1.366576756 = 78.30°$.

- For $\theta_\delta \le \theta \le \theta_\varepsilon$, $\theta_\varepsilon = 2.081741596 = 119.27°$, $\vartheta_2 = \theta_\varepsilon + c_2$, $c_2 = 1.910633236 = 109.47°$, we have

$$\sigma_{rr}^{(0)} = \tfrac{\sqrt{3}}{2}\cos\vartheta_2 - \tfrac{1}{2\sqrt{3}}\cos\vartheta_2\cos 2(\theta-\theta_\beta) + \tfrac{1}{\sqrt{3}}\sin\vartheta_2\sin 2(\theta-\theta_\beta),$$
$$\sigma_{\theta\theta}^{(0)} = \tfrac{\sqrt{3}}{2}\cos\vartheta_2 + \tfrac{1}{2\sqrt{3}}\cos\vartheta_2\cos 2(\theta-\theta_\beta) - \tfrac{1}{\sqrt{3}}\sin\vartheta_2\sin 2(\theta-\theta_\beta),$$
$$\sigma_{r\theta}^{(0)} = \tfrac{1}{2\sqrt{3}}\cos\vartheta_2\sin 2(\theta-\theta_\beta) + \tfrac{1}{\sqrt{3}}\sin\vartheta_2\cos 2(\theta-\theta_\beta).$$

- For $\theta_\varepsilon \le \theta \le \theta_\zeta$, $\theta_\zeta = 2.186257912 = 125.26°$, we have

$$\sigma_{rr}^{(0)} = \tfrac{1}{\sqrt{3}}\cos(\theta+c_2), \quad \sigma_{\theta\theta}^{(0)} = \tfrac{2}{\sqrt{3}}\cos(\theta+c_2), \quad \sigma_{r\theta}^{(0)} = \tfrac{1}{\sqrt{3}}\sin(\theta+c_2).$$

- For $\theta_\zeta \le \theta \le \pi$, we have

$$\sigma_{rr}^{(0)} = -\tfrac{1}{2}(1+\cos 2\theta), \quad \sigma_{\theta\theta}^{(0)} = -\tfrac{1}{2}(1-\cos 2\theta), \quad \sigma_{r\theta}^{(0)} = \tfrac{1}{2}\sin 2\theta.$$

Here the approach developed in [Dong and Pan 1990; Rahman and Hancock 2006; Stepanova 2009b] has been applied. The circumferential distributions of the stress tensor components $\sigma_{ij}^{(0)}(\theta)$ in the neighborhood of the crack tip for $M^p = 0.5$ are given as follows:

- For $-\pi \le \theta \le \theta_\alpha$, $\theta_\alpha = -3.082081755 = -176.60°$, we have

$$\sigma_{rr}^{(0)} = -\tfrac{1}{2}(1+\cos 2\theta), \quad \sigma_{\theta\theta}^{(0)} = -\tfrac{1}{2}(1-\cos 2\theta), \quad \sigma_{r\theta}^{(0)} = \tfrac{1}{2}\sin 2\theta.$$

- For $\theta_\alpha \le \theta \le \theta_\beta$, $\theta_\beta = -2.069949494 = -118.60°$, we have

$$\sigma_{rr}^{(0)} = \tfrac{\sqrt{3}}{2}\cos\vartheta_1 - \tfrac{1}{2\sqrt{3}}\cos\vartheta_1\cos 2(\theta-\theta_\beta) + \tfrac{1}{\sqrt{3}}\sin\vartheta_1\sin 2(\theta-\theta_\beta),$$
$$\sigma_{\theta\theta}^{(0)} = \tfrac{\sqrt{3}}{2}\cos\vartheta_1 + \tfrac{1}{2\sqrt{3}}\cos\vartheta_1\cos 2(\theta-\theta_\beta) - \tfrac{1}{\sqrt{3}}\sin\vartheta_1\sin 2(\theta-\theta_\beta),$$
$$\sigma_{r\theta}^{(0)} = \tfrac{1}{2\sqrt{3}}\cos\vartheta_1\sin 2(\theta-\theta_\beta) + \tfrac{1}{\sqrt{3}}\sin\vartheta_1\cos,$$

  where $\vartheta_1 = \theta_\beta + c_1$, $c_1 = 1.107148718 = 63.43°$.

- For $\theta_\beta \le \theta \le \theta_\gamma$, $\theta_\gamma = 0.988154515 = 56.62°$, we have

$$\sigma_{rr}^{(0)} = \tfrac{1}{\sqrt{3}}\cos(\theta+c_1), \quad \sigma_{\theta\theta}^{(0)} = \tfrac{2}{\sqrt{3}}\cos(\theta+c_1), \quad \sigma_{r\theta}^{(0)} = \tfrac{1}{\sqrt{3}}\sin(\theta+c_1).$$

- For $\theta_\gamma \le \theta \le \theta_\delta$, $\theta_\delta = 2.232478539 = 127.91°$, we have

$$\sigma_{rr}^{(0)} = a + \tfrac{1}{4}(1+\cos 2\theta_\delta)\cos 2(\theta-\theta_\delta) + \tfrac{1}{2}\sin 2\theta_\delta\sin 2(\theta-\theta_\delta),$$
$$\sigma_{\theta\theta}^{(0)} = a - \tfrac{1}{4}(1+\cos 2\theta_\delta)\cos 2(\theta-\theta_\delta) - \tfrac{1}{2}\sin 2\theta_\delta\sin 2(\theta-\theta_\delta),$$
$$\sigma_{r\theta}^{(0)} = -\tfrac{1}{4}(1+\cos 2\theta_\delta)\sin 2(\theta-\theta_\delta) + \tfrac{1}{2}\sin 2\theta_\delta\cos 2(\theta-\theta_\delta),$$

  where $a = \frac{1}{4}(-1+3\cos 2\theta_\delta)$.

- For $\theta_\delta \le \theta \le \pi$, we have

$$\sigma_{rr}^{(0)} = -\tfrac{1}{2}(1+\cos 2\theta), \quad \sigma_{\theta\theta}^{(0)} = -\tfrac{1}{2}(1-\cos 2\theta), \quad \sigma_{r\theta}^{(0)} = \tfrac{1}{2}\sin 2\theta.$$

The circumferential distributions of the stress components $\sigma_{ij}^{(0)}(\theta)$ in the vicinity of the crack tip for $M^p = 0.75$ are given as follows:

- For $-\pi \le \theta \le \theta_\alpha$, $\theta_\alpha = -2.904522467 = -166.42°$, we have

$$\sigma_{rr}^{(0)} = -\tfrac{1}{2}(1+\cos 2\theta), \quad \sigma_{\theta\theta}^{(0)} = -\tfrac{1}{2}(1-\cos 2\theta), \quad \sigma_{r\theta}^{(0)} = \tfrac{1}{2}\sin 2\theta.$$

- For $\theta_\alpha \le \theta \le \theta_\beta$, $\theta_\beta = -1.759907174 = -100.84°$, we have

$$\sigma_{rr}^{(0)} = \tfrac{\sqrt{3}}{2}\cos\vartheta_1 - \tfrac{1}{2\sqrt{3}}\cos\vartheta_1\cos 2(\theta-\theta_\beta) + \tfrac{1}{\sqrt{3}}\sin\vartheta_1\sin 2(\theta-\theta_\beta),$$
$$\sigma_{\theta\theta}^{(0)} = \tfrac{\sqrt{3}}{2}\cos\vartheta_1 + \tfrac{1}{2\sqrt{3}}\cos\vartheta_1\cos 2(\theta-\theta_\beta) - \tfrac{1}{\sqrt{3}}\sin\vartheta_1\sin 2(\theta-\theta_\beta),$$
$$\sigma_{r\theta}^{(0)} = \tfrac{1}{2\sqrt{3}}\cos\vartheta_1\sin 2(\theta-\theta_\beta) + \tfrac{1}{\sqrt{3}}\sin\vartheta_1\cos 2(\theta-\theta_\beta),$$

  where $\vartheta_1 = \theta_\beta + c_1$, $c_1 = 0.6918358137 = 39.64°$.

- For $\theta_\beta \le \theta \le \theta_\gamma$, $\theta_\gamma = 1.119349842 = 64.13°$, we have

$$\sigma_{rr}^{(0)} = \tfrac{1}{\sqrt{3}}\cos(\theta+c_1), \quad \sigma_{\theta\theta}^{(0)} = \tfrac{2}{\sqrt{3}}\cos(\theta+c_1), \quad \sigma_{r\theta}^{(0)} = \tfrac{1}{\sqrt{3}}\sin(\theta+c_1).$$

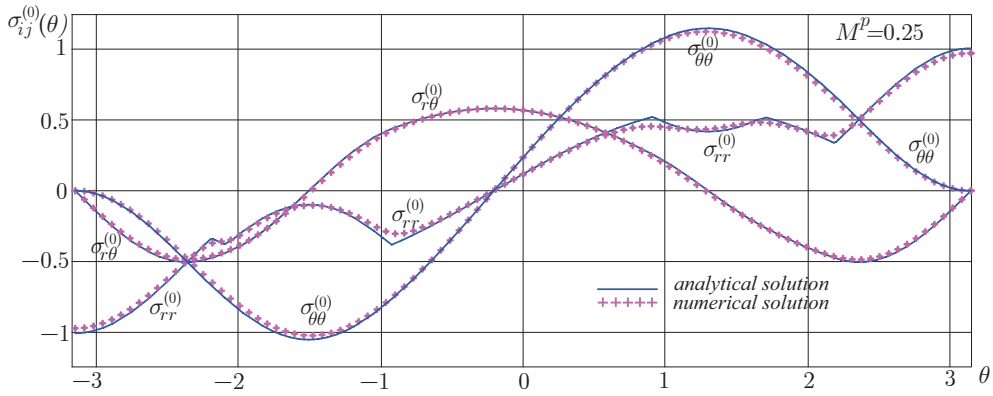

Figure 10. The angular distributions of the stress tensor components in the vicinity of the crack tip for $M^p = 0.25$

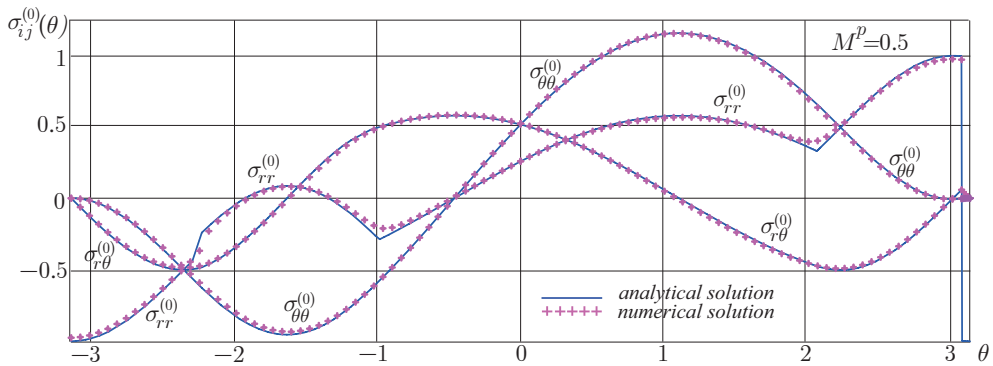

Figure 11. The angular distributions of the stress tensor components in the vicinity of the crack tip for $M^p = 0.5$

- For $\theta_\gamma \le \theta \le \theta_\delta$, $\theta_\delta = 2.385429690 = 136.68°$, we have

$$\sigma_{rr}^{(0)} = a + \tfrac{1}{4}(1+\cos 2\theta_\delta)\cos 2(\theta-\theta_\delta) + \tfrac{1}{2}\sin 2\theta_\delta \sin 2(\theta-\theta_\delta),$$
$$\sigma_{\theta\theta}^{(0)} = a - \tfrac{1}{4}(1+\cos 2\theta_\delta)\cos 2(\theta-\theta_\delta) - \tfrac{1}{2}\sin 2\theta_\delta \sin 2(\theta-\theta_\delta)$$
$$\sigma_{r\theta}^{(0)} = -\tfrac{1}{4}(1+\cos 2\theta_\delta)\sin 2(\theta-\theta_\delta) + \tfrac{1}{2}\sin 2\theta_\delta \cos 2(\theta-\theta_\delta),$$

  where $a = \frac{1}{4}(-1+3\cos 2\theta_\delta)$.

- For $\theta_\delta \le \theta \le \pi$, we have

$$\sigma_{rr}^{(0)} = -\tfrac{1}{2}(1+\cos 2\theta), \quad \sigma_{\theta\theta}^{(0)} = -\tfrac{1}{2}(1-\cos 2\theta), \quad \sigma_{r\theta}^{(0)} = \tfrac{1}{2}\sin 2\theta.$$

The angular distributions of the stress tensor components obtained are shown in Figures 10–12. The data points are numerical results, while the solid lines represent the analytical solution.

One can see from Figures 10–12 that the radial stress $\tilde{\sigma}_{rr}(\theta)$ is continuous at $\theta = 0$. Continuity of the radial stress $\tilde{\sigma}_{rr}(\theta)$ in the limiting case of perfect plasticity confirms the previously accepted assumption.

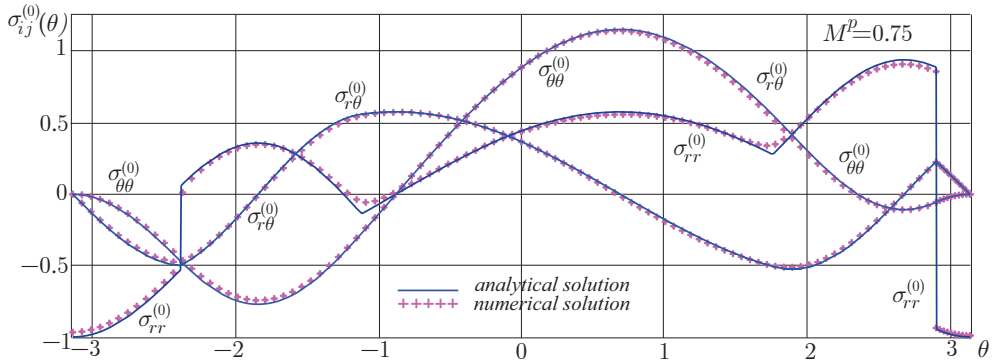

Figure 12. The angular distributions of the stress tensor components in the vicinity of the crack tip for $M^p = 0.75$.

5. Conclusions and discussion of results

In the study the asymptotic analysis and numerical solutions of the nonlinear eigenvalue problems arising from the mixed-mode crack problem in a power law material under plane stress conditions are presented. The method proposed allows us to find the whole spectrum of eigenvalues for a complete range of mixed-mode I/II states of loading from tensile to shear crack problems. The solution is based on the eigenfunction expansion method in the vicinity of the crack tip. The asymptotic presentation of the Airy stress potential reduces the mixed-mode crack problem considered to a nonlinear eigenvalue problem. One eigenvalue corresponding to the pure tensile (mode I) and pure shear (mode II) crack problems is well known and corresponds to the HRR stress field: $\lambda = n/(n+1)$. Following a common practice [Shlyannikov and Kislova 2009; Shlyannikov 2012], it is conventionally assumed that for combined mode I–mode II fracture the eigenvalue corresponding to the HRR problem is the eigenvalue of the nonlinear eigenvalue problem arising from the mixed-mode crack problem. For the case of plane strain conditions, the assumption is valid. The assumption is confirmed by the asymptotic solutions obtained [Shlyannikov and Kislova 2009; Shlyannikov 2012]. However, for the case of plane stress conditions, this hypothesis entails discontinuous radial stress components ahead of the crack tip. All the solutions to the mode I crack and mode II crack problems for plane stress conditions, as well as the solutions for mixed-mode loading [Rahman and Hancock 2006; Shlyannikov and Kislova 2009; Shlyannikov 2012; Stepanova and Adylina 2014], show a continuous radial stress component at $\theta = 0$. In the present paper, it is shown that the mixed-mode loading of the cracked plate results in a new stress singularity around the crack tip. The asymptotic analysis and the numerical calculations performed lead to the new stress field asymptotics in the vicinity of the mixed-mode crack under plane stress conditions. The asymptotic analysis based on the artificial small parameter method of the perturbation theory provided a possibility to reveal the new stress singularity in the vicinity of the crack tip. Next, a technique for numerical determination of the eigenvalues of the nonlinear eigenvalue problem is proposed. Using this technique, the new eigenvalues resulting in continuous radial stress components at $\theta = 0$ are found. It is shown that the method proposed gives the eigenvalues corresponding to the HRR problem in particular cases of mode I and mode II crack problems. The theoretical significance of the present paper is that, from the method described here, one

can clearly know all the mathematically possible distributions of stress singularities at the crack tip under mixed-mode loading.

It is important to develop asymptotic analysis methods and their applications for nonlinear eigenvalue problems in solid mechanics [Andrianov and Awrejcewicz 2013] and, in particular, in nonlinear fracture mechanics and continuum damage mechanics [Barenblatt 2014; Murakami 2012; Voyiadjis 2014], in order to find new and better methods to reliably determine fatigue and fracture behavior. In nonlinear fracture mechanics, the eigenfunction expansion method is one of the most commonly encountered approaches [Murakami 2012; Stepanova 2008a; 2008b; 2009a; Stepanova and Fedina 2008; Stepanova and Igonin 2014]. The method leads to nonlinear eigenvalue problems which stipulate the possible distributions of stress singularities at the crack tip, and the determination of the whole eigenspectrum requires invoking developed asymptotic and computational techniques and their combinations. For instance, it is shown [Stepanova 2008a; 2008b; Stepanova and Igonin 2014] that damage accumulation around the crack tip alters the stress-strain state and results in decreasing the stress singularity in the vicinity of the crack tip. The asymptotic fields in and around the damage zone are quite different from those under K (or J or C^*) dominance in both singularity and distributions. The stress singularity exponent is determined from the nonlinear eigenvalue problem, which needs to be thoroughly solved. The solution of the nonlinear eigenvalue problems provides the solution of the crack problem as a whole. The approach proposed and solutions obtained here can be useful either to find the similarity solutions of the second kind (incomplete similarity) [Barenblatt 2013; 2014; Ritchie 2005] and the solutions of nonlinear eigenvalue problems related to them [Barenblatt 2014; Sih and Tang 2006; Stepanova 2008a; 2008b; Stepanova and Adylina 2014]. It is shown that the meso-mechanical effect of damage accumulation near the crack tip results in new intermediate stress field asymptotic behavior and requires the solution of nonlinear eigenvalue problems. The new eigenvalues can be used for analyzing the near crack tip fields in damaged materials in coupled formulation [Stepanova and Adylina 2014]

In view of the recent research emphases on multiscaling [Tang and Sih 2005; Sih and Tang 2005; 2006; Sih 2008; Stepanova and Igonin 2014], the multiple singularity solution at a point seems to signify the inherent characteristics of micro- and meso-defects. Determination of multiple singularity solutions requires solutions of nonlinear eigenvalue problems. For instance, the model based on the Kachanov–Rabotnov damage evolution law and the power-law of steady-state creep is an example of a problem with the inherent property of incomplete similarity [Stepanova and Adylina 2014]. The method proposed in this paper can be used for the determination of the intermediate asymptotic stress behavior in coupled creep-damage crack problems under mixed-mode loading conditions, since the equations of the problem must have similarity form of the solution and we can derive the solution of the crack problem if the ansatz for the solution of nonlinear eigenvalue problems is obtained. It should be noted also that the class of nonlinear eigenvalue problems arising in nonlinear fracture mechanics is essential in connection with creating multiscale models of fracture [Barenblatt 2013; 2014; Stepanova and Adylina 2014] with multisingularities with different orders at the crack point. A singularity representation scheme has to be considered where the local damage at the different scales will be modeled by different orders of the stress singularities. Different stress singularities can be related to different loading type and severity of material damage.

In [Tang and Sih 2005; Sih and Tang 2005; 2006; Sih 2008], it is elucidated that microscopic effects can have a significant influence on the macroscopic behavior of material. A new approach is needed to

describe the multiscale character of the material microstructure. In [Tang and Sih 2005], a singularity representation scheme where scale effects are modeled by different orders of the stress singularities is proposed. The degree of damage in the vicinity of the crack tip is reflected by the orders of the stress singularities.

In accordance with these models, it is necessary to introduce the hierarchy of the zones in the vicinity of the crack tip with dominating role of different stress asymptotic behavior and to realize the matching procedures between different stress asymptotic solutions. The accurate construction of all the intermediate zones with one or other stress asymptotics requires the knowledge of the whole spectrum of eigenvalues, and these problems are still open.

References

[Akbardoost and Ayatollahi 2014] J. Akbardoost and M. R. Ayatollahi, "Experimental analysis of mixed mode crack propagation in brittle rocks: the effect of non-singular terms", *Eng. Fract. Mech.* **129** (2014), 77–89.

[Andrianov and Awrejcewicz 2013] I. V. Andrianov and J. Awrejcewicz, *Методы асимптотического анализа и синтеза в нелинейной динамике и механике деформируемого твердого тела*, Institute of Computer Investigations, Izhevsk, 2013.

[Andrianov et al. 2014] I. V. Andrianov, J. Awrejcewicz, V. V. Danishevs'kyy, and A. O. Ivankov, *Asymptotic methods in the theory of plates with mixed boundary conditions*, Wiley, Chichester, 2014.

[Barenblatt 2013] G. I. Barenblatt, *Similarity, self-similarity and intermediate asymptotics*, Springer, Berlin, 2013.

[Barenblatt 2014] G. I. Barenblatt, *Flow, deformation and fracture: lectures on fluid mechanics and the mechanics of deformable solids for mathematicians and physicists*, Cambridge Texts in Applied Mathematics **49**, Cambridge University Press, 2014.

[Berto and Lazzarin 2013] F. Berto and P. Lazzarin, "Multiparametric full-field representations of the in-plane stress fields ahead of cracked components under mixed mode loading", *Int. J. Fatigue* **46** (2013), 16–26.

[Berto and Lazzarin 2014] F. Berto and P. Lazzarin, "Recent developments in brittle and quasi-brittle assessment of engineering materials by means of local approaches", *Mater. Sci. Eng. R* **75** (2014), 1–48.

[Botvina et al. 2013] L. R. Botvina, N. A. Chzarkova, M. R. Tutin, A. P. Soldatenkov, Y. A. Demina, and V. P. Levin, "Развитие пластических зон и поврежденности при различных видах нагружения", *Zavod. Lab. Diagn. Mater.* **79**:5 (2013), 46–55. Translated title: "Development of plastic flow zones and damage under various types of loading".

[Bui 2006] H. D. Bui, *Fracture mechanics: inverse problems and solutions*, Springer, Dordrecht, 2006.

[Bui 2011] A. Erlacher and H. Markenscoff (editors), *On duality, symmetry and symmetry lost in solid mechanics: selected works of H. D. Bui*, Presses Ponts et Chaussées, Paris, 2011.

[Constantinescu and Korsunsky 2007] A. Constantinescu and A. Korsunsky, *Elasticity with Mathematica: an introduction to continuum mechanics and linear elasticity*, Cambridge University Press, 2007.

[Decreuse et al. 2012] P. Y. Decreuse, S. Pommier, M. Poncelet, and B. Raka, "A novel approach to model mixed mode plasticity at the crack tip and crack growth. Experimental validations using velocity fields from digital image correlation", *Int. J. Fatigue* **42** (2012), 271–283.

[Dong and Pan 1990] P. Dong and J. Pan, "Asymptotic crack-tip fields for perfectly plastic solids under plane-stress and mixed-mode loading conditions", *J. Appl. Mech.* (*ASME*) **57**:3 (1990), 635–638.

[Hello et al. 2012] G. Hello, M. Ben Tahar, and J.-M. Roelandt, "Analytical determination of coefficients in crack-tip stress expansions for a finite crack in an infinite plane medium", *Int. J. Solids Struct.* **49**:3–4 (2012), 556–566.

[Hutchinson 1968a] J. W. Hutchinson, "Plastic stress and strain fields at a crack tip", *J. Mech. Phys. Solids* **16**:5 (1968), 337–347.

[Hutchinson 1968b] J. W. Hutchinson, "Singular behaviour at the end of tensile crack in a hardening material", *J. Mech. Phys. Solids* **16**:1 (1968), 13–31.

[Kuna 2013] M. Kuna, *Finite elements in fracture mechanics: theory—numerics—applications*, Solid Mechanics and its Applications **201**, Springer, Dordrecht, 2013.

[Leblond and Frelat 2014] J.-B. Leblond and J. Frelat, "Development of fracture facets from a crack loaded in mode I+III: solution and application of a model 2D problem", *J. Mech. Phys. Solids* **64** (2014), 133–153.

[Loghin and Joseph 2001] A. Loghin and P. F. Joseph, "Asymptotic solutions for mixed mode loading of cracks and wedges in power law hardening materials", *Eng. Fract. Mech.* **68**:14 (2001), 1511–1534.

[Loghin and Joseph 2003] A. Loghin and P. F. Joseph, "Mixed mode fracture in power law hardening materials near mode I", *Int. J. Fract.* **123** (2003), 81–106.

[Lomakin and Melnikov 2009] E. V. Lomakin and A. M. Melnikov, "Пластическое плоское напряженное состояние тел, свойства которых зависят от вида напряженного состояния", *Vychisl. Mekh. Splosh. Sred.* **2**:2 (2009), 48–64. English abstract available; translated title: "Plane stress state of media with plastic properties sensitive to the type of stress".

[Lomakin and Melnikov 2011] E. V. Lomakin and A. M. Melnikov, "Задачи плоского напряженного состояния тел с вырезами, пластические свойства которых зависят от вида напряженного состояния", *Izv. Akad. Nauk SSSR Mekh. Tverd. Tela* **46**:1 (2011), 77–89. Translated as "Plane stress state problems for notched bodies whose plastic properties depend on the form of the stress state" in *Mech. Solids* **46**:1 (2011), 62–69.

[Murakami 2012] S. Murakami, *Continuum damage mechanics: a continuum mechanics approach to the analysis of damage and fracture*, Solid Mechanics and its Applications **185**, Springer, Dordrecht, 2012.

[Nayfeh 2000] A. H. Nayfeh, *Perturbation methods*, Wiley, New York, 2000.

[Nayfeh 2011] A. H. Nayfeh, *The method of normal forms*, 2nd ed., Wiley, Weinheim, 2011.

[Ondraček and Materna 2014] J. Ondraček and A. Materna, "FEM evaluation of the dissipated energy in front of a crack tip under 2D mixed mode loading condition", *Procedia Mater. Sci.* **3** (2014), 673–678.

[Pan and Lin 2006] J. Pan and P.-C. Lin, "Analytical solutions for crack-tip sectors in perfectly plastic Mises materials under mixed in-plane and out-of-plane shear loading conditions", *Eng. Fract. Mech.* **73**:13 (2006), 1797–1813.

[Pestrikov and Morozov 2012] V. M. Pestrikov and E. M. Morozov, *Механика разрушения: курс лекций*, EPC Professiya, St. Petersburg, 2012.

[Rahman and Hancock 2006] M. Rahman and J. W. Hancock, "Elastic perfectly-plastic asymptotic mixed mode crack tip fields in plane stress", *Int. J. Solids Struct.* **43**:13 (2006), 3692–3704.

[Rice 1967] J. R. Rice, "Stresses due to a sharp notch in a work hardening elastic-plastic material loaded by longitudinal shear", *J. Appl. Mech.* (*ASME*) **34**:2 (1967), 287–298.

[Rice 1968] J. R. Rice, "Mathematical analysis in the mechanics of fracture", Chapter 3, pp. 191–311 in *Fracture: an advanced treatise*, vol. 2, edited by H. Liebowitz, Academic Press, New York, 1968.

[Rice and Rosengren 1968] J. R. Rice and G. F. Rosengren, "Plane strain deformation near a crack tip in a power-law hardening material", *J. Mech. Phys. Solids* **16**:1 (1968), 1–12.

[Richard et al. 2014] H. A. Richard, B. Schramm, and N.-H. Schirmeisen, "Cracks on mixed mode loading: theories, experiments, simulations", *Int. J. Fatigue* **62** (2014), 93–103.

[Ritchie 2005] R. O. Ritchie, "Incomplete self-similarity and fatigue-crack growth", *Int. J. Fract.* **132**:3 (2005), 197–203.

[Shih 1973] C. F. Shih, *Elastic-plastic analysis of combined mode crack problems*, thesis, Harvard University, Cambridge, MA, 1973.

[Shih 1974] C. F. Shih, "Small scale yielding analysis of mixed mode plane-strain crack problems", pp. 187–210 in *Fracture analysis* (College Park, MD, 1973), vol. 2, ASTM Special Technical Publication **560**, American Society for Testing and Materials, Philadelphia, 1974.

[Shlyannikov 2003] V. N. Shlyannikov, *Elastic-plastic mixed-mode fracture criteria and parameters*, Lecture Notes in Applied Mechanics **7**, Springer, Berlin, 2003.

[Shlyannikov 2012] V. N. Shlyannikov, "Решение задач нелинейного деформирования и разрушения материалов при сложном напряженном состоянии", *Fiz. Mezomekh.* **15**:1 (2012), 57–67. Translated as "Solution of nonlinear strain and fracture problems for materials in complex stress states" in *Phys. Mesomech.* **15**:3–4 (2012), 176–184.

[Shlyannikov 2013] V. N. Shlyannikov, "T-stress for crack paths in test specimens subject to mixed mode loading", *Eng. Fract. Mech.* **108** (2013), 3–18.

[Shlyannikov and Kislova 2009] V. N. Shlyannikov and S. Y. Kislova, "Параметры смешанных форм деформирования для трещины в виде математического разреза", *Izv. Saratov Univ. Mat. Mekh. Inform.* **9**:1 (2009), 77–84. English abstract avaiable; translated title: "Mode mixity parameters for mathematical crack type".

[Shlyannikov and Zakharov 2014] V. N. Shlyannikov and A. P. Zakharov, "Multiaxial crack growth rate under variable T-stress", *Eng. Fract. Mech.* **123** (2014), 86–99.

[Shlyannikov et al. 2014] V. N. Shlyannikov, A. V. Tumanov, and A. P. Zakharov, "The mixed mode crack growth rate in cruiciform specimens subject to biaxial loading", *Theor. Appl. Fract. Mech.* **73** (2014), 68–81.

[Sih 2008] G. C. Sih, "Мезомеханика, понятие сегментации и мультискейлинговый подход: нано-микро-макро", *Fiz. Mezomekh.* **11**:3 (2008), 5–18. Translated as "Birth of mesomechanics arising from segmentation and multiscaling: nano-micro-macro" in *Phys. Mesomech.* **11**:3–4 (2008), 124–136.

[Sih and Tang 2005] G. C. Sih and X. S. Tang, "Scaling of volume energy density function reflecting damage by singularities at macro-, meso- and microscopic level", *Theor. Appl. Fract. Mech.* **43**:2 (2005), 211–231.

[Sih and Tang 2006] G. C. Sih and X. S. Tang, "Simultaneous occurence of double micro/macro stress singularities for multiscale crack model", *Theor. Appl. Fract. Mech.* **46**:2 (2006), 87–104.

[Sliva et al. 2010] G. Sliva, A. Brezillon, J. M. Cadou, and L. Duigou, "A study of the eigenvalue sensitivity by homotopy and perturbation methods", *J. Comput. Appl. Math.* **234**:7 (2010), 2297–2302.

[Smith et al. 2001] D. J. Smith, M. R. Ayatollahi, and M. J. Pavier, "The role of T-stress in brittle fracture for linear elastic materials under mixed-mode loading", *Fatigue Fract. Eng. Mater. Struct.* **24**:2 (2001), 137–150.

[Stepanova 2008a] L. V. Stepanova, "Eigenspectra and orders of stress singularity at a mode I crack tip for a power-law medium", *C. R. Mécanique* **336**:1-2 (2008), 232–237.

[Stepanova 2008b] L. V. Stepanova, "О собственных значениях в задаче о трещине антиплоского сдвига в материале со степенными определяющими уравнениями", *Prikl. Mekh. Tekh. Fiz.* **49**:1 (2008), 173–180. Translated as "Eigenvalues of the antiplane-shear crack problem for a power-law material" in *J. Appl. Mech. Tech. Phys.* **49**:1 (2008), 142–147.

[Stepanova 2009a] L. V. Stepanova, "Анализ собственных значений в задаче о трещине в материале со степенным определяющим законом", *Zh. Vychisl. Mat. Mat. Fiz.* **49**:8 (2009), 1399–1415. Translated as "Eigenvalue analysis for a crack in a power-law material" in *Comput. Math. Math. Phys.* **49**:8 (2009), 1332–1347.

[Stepanova 2009b] L. V. Stepanova, "Асимптотика напряжений и скоростей деформаций вблизи вершины трещины поперечного сдвига в материале, поведение которого описывается дробно-линейным законом", *Prikl. Mekh. Tekh. Fiz.* **50**:1 (2009), 165–176. Translated as "Asymptotics of stresses and strain rates near the tip of a transverse shear crack in a material whose behavior is described by a fractional-linear law" in *J. Appl. Mech. Tech. Phys.* **50**:1 (2009), 137–146.

[Stepanova and Adylina 2014] L. V. Stepanova and E. M. Adylina, "Напряженно-деформированное состояние в окрестности вершины трещины в условиях смешанного нагружения", *Prikl. Mekh. Tekh. Fiz.* **55**:5 (2014), 181–194. Translated as "Stress-strain state in the vicinity of a crack tip under mixed loading" in *J. Appl. Mech. Tech. Phys.* **55**:5 (2014), 885–895.

[Stepanova and Fedina 2008] L. V. Stepanova and M. E. Fedina, "Автомодельное решение задачи о трещине отрыва в связанной постановке", *Prikl. Mat. Mekh.* **72**:3 (2008), 516–527. Translated as "Self-similar solution of a tensile crack problem in a coupled formulation" in *J. Appl. Math. Mech.* **72**:3 (2008), 360–368.

[Stepanova and Igonin 2014] L. V. Stepanova and S. A. Igonin, "Perturbation method for solving the nonlinear eigenvalue problem arising from fatigue crack growth problem in a damaged medium", *Appl. Math. Model.* **38**:14 (2014), 3436–3455.

[Tang and Sih 2005] X. S. Tang and G. C. Sih, "Weak and strong singularities reflecting multiscale damage: micro-boundary conditions for free-free, fixed-fixed and free-fixed constraints", *Theor. Appl. Fract. Mech.* **43**:1 (2005), 5–62.

[Vildeman et al. 2012] V. E. Vildeman, M. P. Tretyakov, T. V. Tretyakova, R. V. Bulbovich, S. V. Babyshkin, A. V. Il'inych, D. S. Lobanov, and A. V. Ipatova, *Экспериментальные исследования свойств материалов при сложных термомеханических воздействиях*, Fizmatlit, Moscow, 2012.

[Vildeman et al. 2014] V. E. Vildeman, E. V. Lomakin, and M. P. Tretyakov, "Закритическое деформирование сталей при плоском напряженном состоянии", *Izv. Akad. Nauk SSSR Mekh. Tverd. Tela* **49**:1 (2014), 26–36. Translated as "Postcritical deformation of steels in plane stress state" in *Mech. Solids* **49**:1 (2014), 18–26.

[Voyiadjis 2014] G. Z. Voyiadjis, *Handbook of damage mechanics: nano to macro scale for materials and structures*, Springer, Berlin, 2014.

[Wei 2010] R. P. Wei, *Fracture mechanics: integration of mechanics, materials science and chemistry*, Cambridge University Press, 2010.

[Wei et al. 2011] Z. Wei, X. Deng, M. A. Sutton, J. Yan, C.-S. Cheng, and P. Zavattieri, "Modeling of mixed-mode crack growth in ductile thin sheets under combined in-plane and out-of-plane loading", *Eng. Fract. Mech.* **78**:17 (2011), 3082–3101.

Received 23 Jul 2014. Revised 6 Nov 2014. Accepted 25 Dec 2014.

LARISA V. STEPANOVA: stepanovalv@samsu.ru
Department of Mathematical Modelling in Mechanics, Samara State University, 1 Akad. Pavlov, Samara, 443011, Russia

EKATERINA M. YAKOVLEVA: adulinaem@samsu.ru
Department of Mathematical Modelling in Mechanics, Samara State University, 1 Akad. Pavlov, Samara, 443011, Russia

JOURNAL OF MECHANICS OF MATERIALS AND STRUCTURES

msp.org/jomms

Founded by Charles R. Steele and Marie-Louise Steele

See msp.org/jomms for submission guidelines.

JoMMS (ISSN 1559-3959) at Mathematical Sciences Publishers, 798 Evans Hall #6840, c/o University of California, Berkeley, CA 94720-3840, is published in 10 issues a year. The subscription price for 2015 is US $565/year for the electronic version, and $725/year (+$60, if shipping outside the US) for print and electronic. Subscriptions, requests for back issues, and changes of address should be sent to MSP.

JoMMS peer-review and production is managed by EditFLOW® from Mathematical Sciences Publishers.

PUBLISHED BY

mathematical sciences publishers

nonprofit scientific publishing

http://msp.org/

Journal of Mechanics of Materials and Structures

Volume 10, No. 3 May 2015

Special issue

In Memoriam: Huy Duong Bui